Reduced quantum electrodynamics in curved space

P. I. C. Caneda[*]
Centro Brasileiro de Pesquisas Físicas, 222990-180 Rio de Janeiro, RJ, Brazil

G. Menezes[†]
Centro Brasileiro de Pesquisas Físicas, 222990-180 Rio de Janeiro, RJ, Brazil and Departamento de Física, Universidade Federal Rural do Rio de Janeiro, 23897-000 Seropédica, RJ, Brazil

(Received 2 December 2020; accepted 23 February 2021; published 22 March 2021)

An approach that has been given promising results concerning investigations on the physics of graphene is the so-called reduced quantum electrodynamics. In this work we consider the natural generalization of this formalism to curved spaces. We employ the local momentum space representation. We discuss the validity of the Ward identity and study one-loop diagrams in detail. We show that the one-loop beta function is zero. As an application, we calculate the one-loop optical conductivity of graphene by taking into account curvature effects which can be incorporated locally. In addition, we demonstrate how such effects may contribute to the conductivity. Furthermore, and quite unexpectedly, our calculations unveil the emergence of a curvature-induced effective chemical potential contribution in the optical conductivity.

DOI: 10.1103/PhysRevD.103.065010

I. INTRODUCTION

In the last decades condensed-matter systems of diverse natures have been increasingly studied under the methods of quantum field theory (QFT). This has emerged as an important tool in the condensed-matter community in the sense that QFT allows us to theoretically explore the prominent physics developing on the relevant low-energy scale probed in experiments. Remarkably, it has also been realized that elusive particles that appear in the context of high-energy physics, such as Weyl and Majorana fermions, can naturally emerge in the form of quasiparticles in a condensed-matter setting [1,2]. On the other hand, recently one has witnessed the outbreak of investigations dedicated to collectively understand the prospects of exploiting condensed-matter models as possible experimental realizations of physical situations that arise in the context of general relativity and of quantum field theories in curved backgrounds. For instance, it now has been well established that kinematic aspects of black holes can be investigated in weakly interacting Bose gases [3]. In this analog model configuration, theoretical surveys have also probed aspects of interesting kinematical effects that arise in classical and quantum systems, such as, for example, phenomena involving superradiance processes [4].

The investigation proposed here considers this current trend to borrow concepts originally developed in high-energy physics for the study of low-energy systems commonly found in condensed matter. We are particularly interested in the transport properties of graphene. The low-energy physics of two-dimensional carbon systems [5,6] is governed by the presence of two generations of massless Dirac fermions. The electronic interactions in Dirac liquids lead to a wealth of intriguing transport phenomena which have attracted a fair amount of attention since the first synthesization of graphene in 2004 [7]. Indeed, recent experiments uncover the relevance of such electronic interactions at low temperatures [8–11]. In turn, the interplay between strong Coulomb interactions and weak quenched disorder in graphene has also been elucidated, and the general expectation is that vector-potential disorder may play a key role in the description of transport in suspended graphene films [12]. Motivated by clear evidence of the strongly coupled nature of graphene, transport coefficients were calculated within a modern holographic setup [13].

The specific structure of the $2D$ crystal lattice permits graphene systems to be viable settings to study some of the interesting effects which arise in QFT in curved space-times [14–16]. In this context, measurable effects of QFT in a curved-background description of the electronic properties of graphene represent a growing ongoing line of research. A number of proposals to interpret several observed effects in graphene sheets such as curved ripples [17], corrugations [18], pure strain configurations [19] and even nonuniform elastic deformations [20] in the light of a curved-space description of the electronic properties of graphene has

[*]caneda@cbpf.br
[†]gabrielmenezes@ufrrj.br

occupied much of the contemporary associated literature. The appearance of gauge fields in graphene systems has also made it possible to establish a firm bridge between the physics of graphene and gravity-like phenomena allowing the unification of concepts from elasticity and cosmology [21].

The chiral nature of the charge carriers in graphene is responsible for the existence of a minimal ac conductivity in the collisionless regime which is universal [22]. In this respect much theoretical effort has been devoted to understand the effects of electronic interactions on the optical conductivity in such a scenario (for an interesting discussion, see Ref. [23] and references cited therein). One possible framework with which one can address this issue is given by the so-called reduced quantum electrodynamics (RQED). This is a quantum field theory describing the interaction of an Abelian $U(1)$ gauge field with a fermion field living in flat space-times with different dimensions [24,25]. Motivations for the investigation of such reduced theories comprise their feasible application in low-dimensional condensed-matter settings, in particular graphene systems. Indeed, it has been claimed that calculations within the formalism of RQED reproduce as close as possible the experimental results for the minimum conductivity of graphene [26]. Electromagnetic current correlation has also been computed within the context of RQED [27]. Other interesting, noteworthy features of RQED include the validity of the Coleman-Hill theorem and the existence of quantum scale invariance [28,29]. For recent studies of chiral symmetry breaking in RQED at finite temperature and in the presence of a Chern-Simons term, see Refs. [30,31].

In the present exploration our theoretical laboratory will be the generalization of the formalism of RQED to curved spaces. We do not wish to single out one particular metric in our exploration, but instead we will keep our discussion to general spatial geometries. For that we will use a momentum-space representation of the Feynman propagator in arbitrary curved space-times [32,33]. As usual the construction rests upon the usage of Riemann normal coordinates [34,35]. As an application, our discussion will allow us to calculate the one-loop high-frequency behavior of the optical conductivity in the presence of curvature effects in graphene by using the Kubo formula. We will demonstrate that the effect of the curvature upon the optical conductivity, to a certain extent, is to induce the appearance of an effective chemical potential when the Ricci scalar is positive. We will also explore the intriguing possibility that such curvature effects can actually contribute to an increase in the conductivity of graphene. We employ units such that $\hbar = c = 1$.

II. RQED IN CURVED SPACE

A. RQED in flat space

Let us begin our discussion in flat space. Massless Dirac electrons are assumed to interact via the RQED in two spatial dimensions. Such a model in flat space is given by the following action[1] (for the Euclidean version, see Ref. [26]):

$$S = \int d^{d_\gamma}x\left[-\frac{1}{4}F_{\mu\nu}F^{\mu\nu} - \frac{1}{2\xi}(\partial_\mu A^\mu)^2\right] + \int d^{d_e}x\left(\bar{\psi}_A i v_F \not{\partial}\psi_A - \eta^{\alpha\beta} j_\alpha A_\beta\right) \tag{1}$$

where $x^0 = v_F t$ and $j^\mu = e\bar{\psi}_A\gamma^\mu\psi_A = e(\bar{\psi}_A\gamma^0\psi_A, v_F\bar{\psi}_A\gamma^i\psi_A)$, $i = 1, 2$. In such expressions, ψ_A is a 2-component Dirac field, $\bar{\psi}_A = \psi_A^\dagger\gamma^0$ is its adjoint, $F_{\mu\nu} = \partial_\mu A_\nu - \partial_\nu A_\mu$, γ^μ are rank-2 Dirac matrices given by $\gamma^0 = \sigma^3$, $\gamma^1 = i\sigma^2$, $\gamma^2 = -i\sigma^1$, satisfying $\{\gamma^\mu, \gamma^\nu\} = 2\eta^{\mu\nu}$, with σ_j being the usual Pauli matrices. Also, A denotes a flavor index, specifying the spin component and the valley to which the charge carrier belongs. Since the natural velocity in the gauge sector is that of light, whereas the one occurring in the fermionic sector is the Fermi velocity v_F, Lorentz invariance is broken. An $SU(4)$ version of this model has been recently used to study dynamical gap generation and chiral symmetry breaking in graphene [36].

The above action describes the interaction between a fermion field in d_e dimensions with a gauge field in d_γ dimensions, with $d_e < d_\gamma$. Specifically for our purposes $d_\gamma = d + 1$ and $d_e = (d-1) + 1$. In addition, the indices run as follows: For the first term $\mu = 0, 1, \ldots, d$, and for the second term $\mu = \mu_e = 0, 1, \ldots, (d-1)$. For the case of graphene, $d = 3$. Equation (1) can also be written as

$$S = \int d^{d_\gamma}x\left[-\frac{1}{4}F_{\mu\nu}F^{\mu\nu} - \frac{1}{2\xi}(\partial_\mu A^\mu)^2 + \left(\bar{\psi}_A i v_F \not{\partial}\psi_A - \eta^{\alpha\beta} j_\alpha A_\beta\right)\delta(x^{d_\gamma - d_e})\right] \tag{2}$$

and then the conserved current is defined as

$$j^\mu(x) = e\bar{\psi}_A\gamma^\mu\psi_A\delta(x^{d_\gamma - d_e}), \qquad \mu = \mu_e \tag{3}$$

and the other components are zero. In this work, we will be particularly interested in an alternative model; this corresponds to a vanishing space-time anisotropy and describes the IR Lorentz invariant fixed point where $v_F \to 1$ and the interaction is fully retarded (for a complete discussion see Ref. [37]). To consider the situation away from this fixed point, one should consider the replacement $\gamma^i \to v_F\gamma^i$.

By integrating out the degrees of freedom transverse to the d_e-dimensional space, one obtains the gauge propagator on the plane, which for the case of graphene reads

[1]To avoid cluttering notation the space-time indices of both dimensions are labeled equally, their range is left implicit from their corresponding action.

$$D_{0\mu\nu}(p^2) = \frac{-i}{2\sqrt{p^2}}\left[\eta_{\mu\nu} - \frac{1-\xi}{2}\frac{p_\mu p_\nu}{p^2}\right]. \tag{4}$$

It is possible to introduce now a $d = 3$ gauge field $\tilde{A}_\mu$ on the plane that propagates like Eq. (4). The resulting theory is the RQED mentioned above, also known as pseudo-quantum electrodynamics (PQED) [24]

$$S = \int d^3x\left[-\frac{1}{2}\tilde{F}_{\mu\nu}\frac{1}{\sqrt{-\Box}}\tilde{F}^{\mu\nu} - \frac{1}{2\tilde{\xi}}\partial_\mu\tilde{A}^\mu\frac{1}{\sqrt{-\Box}}\partial_\nu\tilde{A}^\nu + \bar{\psi}_A i v_F \not{\partial}\psi_A - \eta^{\alpha\beta} j_\alpha \tilde{A}_\beta\right]. \tag{5}$$

Actions (1) and (5) are physically equivalent. Whether one should employ one or the other depends on the situation. The mixed-dimensional (1) is adequate for position space methods whereas action (5) is better suited for momentum space techniques. However for the purpose of perturbation theory in momentum space it suffices to derive the propagator (4) without knowledge of (5).

B. RQED in curved space

In this paper we are interested in the curved-space version of the Lorentz invariant fixed-point model. That is

$$S = \int d^{d_\gamma}x\sqrt{-g}\left[-\frac{1}{4}F_{\mu\nu}F^{\mu\nu} - \frac{1}{2\xi}(\nabla_\mu A^\mu)\right] + \int d^{d_e}x\sqrt{-H}\bar{\psi}_A i\gamma^\mu(x)(\partial_\mu + \Omega_\mu + ieA_\mu)\psi_A. \tag{6}$$

where $F_{\mu\nu} = \nabla_\mu A_\nu - \nabla_\nu A_\mu = \partial_\mu A_\nu - \partial_\nu A_\mu$ (the connection terms cancel), $\gamma^\mu(x) = e_a{}^\mu(x)\gamma^a$, $(\Omega_\mu)^\beta{}_\alpha = (1/2)\omega_\mu{}^{ab}(J_{ab})^\beta{}_\alpha$, $(J_{ab})^\beta{}_\alpha$ being the Lorentz generators in spinor space, and $\omega_\mu{}^a{}_b = e_b{}^\nu(-\delta^\lambda{}_\nu\partial_\mu + \Gamma^\lambda{}_{\mu\nu})e^a{}_\lambda$ is the spin connection, whose relation to the Christoffel connection comes from the metricity condition: $\nabla_\mu e^a{}_\nu = \partial_\mu e^a{}_\nu - \Gamma^\lambda{}_{\mu\nu}e^a{}_\lambda + (\omega_\mu)^a{}_b e^b{}_\nu = 0$. We have introduced the vielbein $e^a{}_\lambda$, which satisfies $\eta_{ab}e^a{}_\mu e^b{}_\nu = g_{\mu\nu}$. In addition, $H_{\alpha\beta}$ is the induced metric on the boundary of the space-time with metric $g_{\mu\nu}$. Besides the hypothesis of weak curvatures made in Sec. III, the formalism presented here can be elaborated without fixing a particular form to the metric. That said, for application to the specific case of graphene, one usually considers metrics in a normal Gaussian-coordinate form, that is (in four space-time dimensions)

$$g_{\mu\nu}dx^\mu dx^\nu = dt^2 - dz^2 - h_{ij}dx^i dx^j \tag{7}$$

where $i, j = 1, 2$. In this case,

$$\int d^{d_\gamma}x\sqrt{-g} = \int dt\int dz\int dx^1 dx^2\sqrt{h}$$

where h is the determinant of the spatial metric h_{ij}. Henceforth we will consider this form for the metric in the subsequent calculations.

Equation (6) can also be written in a form similar to Eq. (2), so that the conserved current will have an expression similar to (3). However, one can also consider an alternative form that will be useful in what follows. Define

$$\bar{e}^a{}_\mu(x) = \begin{cases} e^a{}_\mu(x)\delta(x^{d_\gamma - d_e}) & a, \mu = \mu_e \\ 0 & a, \mu = d_e, \ldots, d_\gamma - 1. \end{cases} \tag{8}$$

In the case of graphene, $x^{d_\gamma - d_e} = z$, see Eq. (7). Moreover, we consider that the extra dimensions $d_\gamma - d_e$ are all flat which justifies the usage of the standard Dirac delta function. In this way the action displays a form which closely resembles the one of the standard QED in curved space, namely

$$S = \int d^{d_\gamma}x\sqrt{-g}\left[-\frac{1}{4}F_{\mu\nu}F^{\mu\nu} - \frac{1}{2\xi}(\nabla_\mu A^\mu) + \bar{\psi}_A i\bar{\gamma}^\mu(x)(\partial_\mu + \Omega_\mu + ieA_\mu)\psi_A\right] \tag{9}$$

where $\bar{\gamma}^\mu(x) = \bar{e}_a{}^\mu(x)\gamma^a$. Action (9) will be the starting point of our analysis. In order to carry a one-loop analysis our first goal is to derive a curved space version of propagator (4). This is done in Sec. III where we also discuss in the end the possibility to generalize the PQED action (5) itself.

C. Ward Identity for curved space RQED

Consider the path-integral formulation of the theory, whose generating functional is given by

$$Z = \int DA_\mu D\psi D\bar{\psi} \times \exp\left\{iS + i\int d^{d_\gamma}x\sqrt{-g}(J^\mu A_\mu + \bar{\eta}\psi + \bar{\psi}\eta)\right\} \tag{10}$$

where S is given by (9). There should be also the contribution of the Faddeev-Popov ghost fields to the generating functional which is important in the evaluation of the one-loop effective action; since they will not play a role in our investigation, we choose to omit them for brevity.

Using functional methods, it is not difficult to exhibit the Schwinger-Dyson equation for the fermion propagator:

$$-iS^{-1}(x, x') = -iS_0^{-1}(x, x') + i\Sigma(x, x') \tag{11}$$

where S_0 is the free curved-space counterpart of the fermion propagator and the self-energy reads

$$-i\Sigma(x,x') = \int d^{d_\gamma}z\sqrt{-g(z)} \times \int d^{d_\gamma}u\sqrt{-g(u)}(-ie\gamma^\mu(x)) \times iS(x,u)(-ie\Gamma^\nu(u,x';z))iG_{\mu\nu}(z,x) \quad (12)$$

with $G_{\mu\nu}$ being the exact gauge propagator. In addition, $\Gamma^\nu(u,x';z)$ is the exact three-point function with the external exact propagator removed:

$$\Gamma^\nu(u,x';z) = \frac{\delta^3\Gamma}{\delta A_\nu(z)\delta\psi(u)\delta\bar{\psi}(x')} \quad (13)$$

where Γ is the proper vertex and the functional derivatives are taken with respect to the so-called classical fields. The inverse fermion propagator can also be given as

$$S^{-1}(x,x') = \frac{\delta^2\Gamma}{\delta\psi(x)\delta\bar{\psi}(x')}. \quad (14)$$

The derivation of the Schwinger-Dyson equation for the gauge propagator follows along similar lines; one finds

$$-iG^{-1}_{\mu\nu}(x,x') = -iG^{-1}_{0\mu\nu}(x,x') - i\Pi_{\mu\nu}(x,x') \quad (15)$$

where $G_{0\mu\nu}$ is the free gauge propagator in curved space. The vacuum polarization is defined as

$$i\Pi^{\mu\nu}(x,x') = -\int d^{d_\gamma}y\sqrt{-g(y)}\int d^{d_\gamma}y'\sqrt{-g(y')} \times \mathrm{Tr}[(-ie\gamma^\mu(x))iS(x,y)(-ie\Gamma^\nu(y,y';x')) \times iS(y',x)]. \quad (16)$$

QED in curved space-time has been discussed in several places in the literature, see for instance Refs. [38–40] and the monograph [41]. In turn, a proof of the Ward-Takahashi identity for QED in curved space can be found, for instance, in Ref. [42]. In the present case we can follow a similar procedure. Namely, let A_μ change by $\nabla_\mu\varphi(x)$. This amounts to consider a change in $\bar{\psi}$ and ψ,

$$\bar{\psi}(x) \to e^{-ie\varphi(x)}\bar{\psi}(x).$$

This implies the following change in $S^{-1}(x,x')$:

$$\delta S^{-1}(x,x') = e\int d^{d_\gamma}y\sqrt{-g(y)}\varphi(y)\nabla_\mu\Gamma^\mu(x,x';y). \quad (17)$$

But $\delta S^{-1}(x,x')$ can also be calculated from the transformation for in $\bar{\psi}$ and ψ, which gives

$$\delta S^{-1}(x,x') = ie\int d^{d_\gamma}y\sqrt{-g(y)}\varphi(y)[\delta(x,y) - \delta(x',y)] \times S^{-1}(x,x') \quad (18)$$

where $\delta(x,y) = (-g(y))^{-1/2}\delta^{d_\gamma}(x-y)$. Comparing both expressions, one arrives at the Ward-Takahashi identity

$$\nabla_\mu\Gamma^\mu(x,x';y) = i[\delta(x,y) - \delta(x',y)]S^{-1}(x,x'). \quad (19)$$

Simple usage of the definition of the vacuum polarization together with Eq. (19) leads us to the Ward identity in curved space:

$$\nabla^{x'}_\nu\Pi^{\mu\nu}(x,x') = 0. \quad (20)$$

This derivation certainly holds for the model defined by the action (9). But since this is equivalent to the action given by Eq. (6), the validity of the Ward identity for RQED in curved space is hence established.

III. LOCAL MOMENTUM SPACE REPRESENTATION

A. QED$_4$

In order to deal with the curved propagators, we employ Riemann normal coordinates (RNC) with origin at the point x' [43]. This point is fixed and all other points will be in a normal neighborhood of x'. This means that, in the loop expressions to follow, x is free to vary in a normal neighborhood of the fixed point x'. At the same time we make a Schwinger-DeWitt proper time expansion for the fermion and gauge propagators. Together with the RNC this leads to the so-called local momentum space representation. The usefulness of the local momentum space representation is twofold. The first, practical reason, is that it yields to the standard momentum space techniques because only flat space-time quantities enter due to the RNC expansion. The second, most relevant and physical, is that it carries some nonperturbative information due to a partial resummation of the scalar curvature. Here we give a qualitative overview of this approach to contextualize later discussions and comments. The detailed derivation of the fermionic and gauge propagators are deferred to the appendixes. See also Refs. [44,45].

We begin setting up the wave equations obeyed by the propagators $G^i{}_j(x,x')$ [46]

$$[\delta^i_k\nabla^\mu\nabla_\mu + Q^i{}_k(x)]G^k{}_j(x,x') = \vartheta\delta^i_j\delta(x,x') \quad (21)$$

where the indices i, j indicate any appropriate indices carried by the fields of interest (spinor or vector), $\vartheta = +1$ for the gauge field and $\vartheta = -1$ for the spinor field. $Q^i{}_k(x)$ is a function with indices of the indicated type, and, as above, $\delta(x,x') = |g(x)|^{-1/2}\delta(x-x')$. Moreover, the

covariant derivative in the above expression acts upon the x-dependence of the Green's function and is defined by

$$\nabla_\mu G^i{}_j(x,x') = \partial_\mu G^i{}_j(x,x') + \Gamma_\mu{}^i{}_k(x) G^k{}_j(x,x') \tag{22}$$

where $\Gamma_\mu{}^i{}_k$ is the appropriate connection for the given spin. For the free gauge field in the Feynman gauge, Eq. (21) is simply

$$[\eta_{\mu\lambda}\Box + R_{\mu\lambda}] G^\lambda{}_{\nu'} = \eta_{\mu\nu'}\delta(x,x') \tag{23}$$

so we see that $Q^\mu{}_\nu = R^\mu{}_\nu$. The free massless spinor field satisfies the equation

$$i\gamma^\mu \nabla_\mu S_0(x,x') = \delta(x,x'). \tag{24}$$

However, defining $S_0(x,x') = i\gamma^\mu \nabla_\mu G(x,x')$ and using the identity [46]

$$\gamma^\mu\gamma^\nu\nabla_\mu\nabla_\nu\Psi = \left(\Box + \frac{1}{4}R\right)\Psi$$

where Ψ is any appropriate test function, one obtains that

$$\left(\Box + \frac{1}{4}R\right) G(x,x') = -\delta(x,x'). \tag{25}$$

So we observe that $Q^i{}_j = \delta^i_j R/4$, where i, j are now spinor indices. Indeed, $G(x,x')$ is a bispinor.

Let us first discuss the Riemann normal coordinates expansion. In simple terms it amounts to the application of the equivalence principle on some point x'. This allows a strictly flat space-time description on x' where the standard methods of field theory are valid. For points within the normal neighborhood of x' we pick corrections that are polynomial in the curvature tensors and their derivatives computed at x'.

The Schwinger-DeWitt expansion on the other hand is done directly on the fields' propagators. It makes use of the fact that $G(x,x')$ is a transition amplitude $\langle x,s|x',0\rangle$ evolving under a Schrödinger equation from proper time $\tau = 0$ to $\tau = s$. For $x \to x'$ we fall into the domain of validity of the RNC expansion, which ultimately leads to the following fermionic and gauge propagators (see appendixes)

$$\begin{aligned} S_0(x,x') = \int \frac{d^D k}{(2\pi)^D} e^{-iky} \Bigg[& \frac{\gamma^\nu k_\nu}{k^2 - M_e^2} \\ & + \frac{1}{(k^2 - M_e^2)^2}\left(\frac{1}{2}R_{\nu\rho}\gamma^\nu k^\rho - \frac{\gamma^\nu k_\nu}{6}R\right) \\ & + \frac{2}{3}\frac{\gamma^\nu k_\nu k^\sigma k^\rho R_{\rho\sigma}}{(k^2 - M_e^2)^3} + \cdots \Bigg] \\ D_{0\mu\nu'}(x,x') = -\int \frac{d^{d_\gamma} k}{(2\pi)^{d_\gamma}} e^{-iky} \Bigg[& \frac{\eta_{\mu\nu'}}{k^2 - M_\gamma^2} \\ & + \frac{1}{(k^2 - M_\gamma^2)^2}\left(\frac{2}{3}R_{\mu\nu'} - \frac{1}{6}R\eta_{\mu\nu'}\right) \\ & - \frac{2}{3}\frac{(2R_{\mu\alpha\beta\nu'} - R_{\alpha\beta}\eta_{\mu\nu'})k^\alpha k^\beta}{(k^2 - M_\gamma^2)^3} + \cdots \Bigg]. \end{aligned} \tag{26}$$

In the above $M_e^2 = R(x')/12$ and $M_\gamma^2 = -R(x')/6$ are the result of a nonperturbative resummation. Some comments are in order. First notice that $R(x')$ being computed at x' is formally a number. Furthermore since this is a semiclassical approximation neither M_e^2 nor M_γ^2 are subject to renormalization. Finally we must be careful before interpreting the poles at M_e^2 and M_γ^2 as physical masses because for a generic curved space-time there is no unambiguous split between positive and negative frequencies to define one-particle states. For instance our general proof of the Ward Identity guarantees that there is no conflict between the parameter M_γ and gauge invariance.

Obviously, the local-momentum space representation provides only a local approximation to the propagator. However, it should give reasonable approximate results as long as curvature effects remain weak. It is in this sense that the expression for the optical conductivity to be calculated later on is to be regarded as a high-frequency expansion.

B. Reduced QED

Up until now our discussion parallels the one for standard curved QED_4. We still need to reduce the gauge sector down to $(2+1)$ dimensions. This is a difficult task for a general curved space-time, but within the regime of validity of the local momentum space representation it can be done in the exact same fashion as in the flat space-time case. We find to first order in the Feynman gauge

$$D_{0\mu\nu'}(k^2) = \frac{-i\eta_{\mu\nu'}}{2(k^2 - M_\gamma^2)^{1/2}}. \tag{27}$$

This is the propagator we shall employ in the following one-loop analysis.

In a general gauge the gauge field propagator in QED_4 is to first order in the local momentum space representation[2]

$$D_{0\mu\nu'}(k^2) = \frac{-i}{k^2 - M_\gamma^2}\left[\eta_{\mu\nu'} - (1-\xi)\frac{k_\mu k_{\nu'}}{k^2 - M_\gamma^2}\right]. \quad (28)$$

Within this approximation we find upon projection

$$D_{0\mu\nu'}(k^2) = \frac{-i}{(k^2 - M_\gamma^2)^{1/2}}\left[\eta_{\mu\nu'} - (1-\tilde{\xi})\frac{k_\mu k_{\nu'}}{k^2 - M_\gamma^2}\right]. \quad (29)$$

It is not straightforward, if possible at all, to infer a purely $(2+1)$-dimensional action that reproduces (29) in analogy to the passage from (4) to (5)—i.e., a curved space generalization to PQED. Furthermore, if indeed possible this would only be an UV limit of curved PQED. Finally we notice this is the reason for choosing the name curved RQED instead of curved PQED for the approach we adopt in this work.

IV. ONE-LOOP ANALYSIS

In this work we are interested in calculating the one-loop diagrams:

$$\begin{aligned} i\Pi_1^{\mu\nu}(x,x') &= -\mathrm{Tr}[(-ie\gamma^\mu(x))iS_0(x,x')(-ie\gamma^\nu(x'))iS_0(x',x)] \\ -i\Sigma_1(x,x') &= (-ie\gamma^\mu(x))iS_0(x,x')(-ie\gamma^\nu(x'))iD_{0\mu\nu}(x',x) \\ -ie\Gamma^\mu(y,y';x) &= (-ie\gamma^\beta(x))iS_0(x,y)(-ie\gamma^\mu(y))iS_0(x,y')(-ie\gamma^\alpha(y'))iD_{0\alpha\beta}(y',y) \end{aligned} \quad (30)$$

where $D_{0\mu\nu}$ are the (free) curved-space counterpart of the reduced gauge field propagators, respectively. The one-loop fermion propagator is then given by

$$\begin{aligned} iS(x,x') = {} & iS_0(x,x') \\ & + \int d^{d_\gamma}z\sqrt{-g(z)}\int d^{d_\gamma}z'\sqrt{-g(z')} \\ & \times iS_0(x,z)(-i\Sigma_1(z,z'))iS_0(z',x'). \end{aligned} \quad (31)$$

As standard in QFT calculations, some of such integrals are divergent, and a careful procedure of regularization and renormalization should be taken into account. As quoted above, quantum electrodynamics in curved space has been considerably discussed in the literature [38–42]. Following [27], we employ dimensional regularization. Loop integrals will depend on d_e which is given as a function of suitable quantities ϵ_γ and ϵ_e:

$$d_e = 4 - 2\epsilon_\gamma - 2\epsilon_e.$$

After evaluating the loop integrals for a general d_e, we employ the above expression for a fixed value of ϵ_e, namely $\epsilon_e = 1/2$. The associated divergences will correspond to poles in $1/\epsilon_\gamma$. The relation between bare and renormalized quantities follows the usual recipe,

$$\begin{aligned} \psi &= Z_2^{1/2}\psi_R \\ A &= Z_3^{1/2}A_R \\ e &= Z_e e_R = \frac{Z_1}{Z_2 Z_3^{1/2}}e_R \\ \Gamma_R^\mu &= Z_1^{-1}\Gamma^\mu \\ \xi &= Z_3\xi_R \end{aligned} \quad (32)$$

where the subscript R means a renormalized quantity. As usual, a renormalization scale $\tilde{\mu}$ with dimensions of mass must be introduced. One then rewrites the Lagrangian density in terms of such renormalized quantities and renormalization constants that absorb all UV divergences. Use of the Ward-Takahashi identity (19) leads to $Z_1 = Z_2$. In the modified minimal subtraction scheme (which we adopt here) the renormalization constants take a simple form

$$Z_n = 1 + \delta Z_n(\alpha_R, \epsilon_\gamma), \quad n = 1, 2, 3 \quad (33)$$

where $\alpha_R = e_R^2/4\pi$ is the renormalized fine-structure constant and $\delta Z_n(\alpha_R, \epsilon_\gamma)$ is expanded in powers of α_R and $1/\epsilon_\gamma$. Taking into account such an expression for the renormalization constants, one obtains a counterterm Lagrangian density (besides a Lagrangian density written in terms of only the renormalized fields and parameters).

A theorem proved by Collins states that all counterterms are necessarily local in a flat background [47]. An important consequence of this theorem is that a nonlocal contribution in the action does not get renormalized (i.e., the associated $\delta Z = 0$). This point is extensively discussed in Ref. [23]. In the case of RQED in flat space, this implies that the beta function is zero to all orders in perturbation theory, producing thereby an explicit example of an interacting boundary conformal field theory. On the other

[2]Propagator (28) seems to break gauge invariance upon contracting with p^μ as there is a leftover proportional to M_γ^2. This is in no contradiction with our general result for gauge invariance in Sec. II C. To understand the issue one must notice that the leftover is of higher order in the local momentum space expansion (26). Inspecting the corresponding higher order contribution reveals a canceling term.

hand, since the discussion in Ref. [47] was based on the analysis of superficial degree of divergence of Feynman diagrams, in a general curved space, when one combines the local-momentum representation and the usual Feynman technique, one obtains that the necessary counterterms must also be covariant local expressions. This is because divergences in loops should be tantamount to local effects. However, one can argue that propagators represent correlations of fields at different space-time points, so one must be able to obtain nonlocal contributions. Indeed, these arise from the finite parts of the loops, but not from the UV divergences. The uncertainty principle lies underneath this split: Ultraviolet divergences must be associated with the high-energy contribution and hence emerge as short-distance (local) effects. This should also hold in curved space-times, even if the theory contains some nonlocal operators. That is why one should naturally expect that nonlocal contributions in the curved-space action will not get renormalized. In particular, this suggests that the beta function of curved-space RQED should also be zero to all orders in perturbation theory. The one-loop proof of this statement will be given in due course.

A. One-loop fermion self-energy

Now we turn to the task of studying the one-loop diagrams in detail. We start our discussion with the fermion self-energy. This is given by the second expression in Eq. (30), see also Fig. 1. Considering Riemann normal coordinates with origin at x', one must insert into such an expression the propagators calculated in the appendixes, which are given as expansions in the curvatures. Concerning the gauge propagator, and as discussed above, one should integrate out the gauge degrees of freedom transverse to the d_e-dimensional space in which the fermion lives. This amounts to consider an integration over the $d_\gamma - d_e$ bulk degrees of freedom of the gauge propagator, whose expression is derived in Appendix C. After specializing to $d_e = (2+1)$-dimensional case, one finds the following local-momentum representation for the one-loop fermionic self-energy:

$$\Sigma_1(k,x') = \frac{1}{2}\int \frac{d^3q}{(2\pi)^3}(-ie\gamma^\mu)\frac{i(\not{k}-\not{q})}{(k-q)^2 - M_e^2 + i\epsilon}(-ie\gamma^\nu) \times \frac{i\eta_{\mu\nu}}{(q^2 - M_\gamma^2 + i\epsilon)^{1/2}}. \tag{34}$$

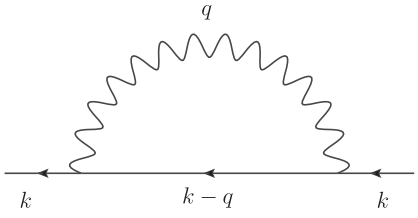

FIG. 1. One-loop fermion self-energy.

where, as defined in the appendixes, $M_e^2 = R(x')/12$ and $M_\gamma^2 = -R(x')/6$. As is clear from the above expression, we are working in the Feynman gauge, $\xi = 1$. Moreover, notice that we kept only the leading-order terms in the expansion in curvatures for the propagators. These are the only ones that will generate a divergence at $d_e = 3$ and hence to a $\tilde{\mu}$ dependence. Accordingly, we also kept only the leading-order term in the expansion of the gamma matrices, so the γ's in the above equation are just the standard flat-space gamma matrices in three dimensions. Finally, observe the introduction of the $i\epsilon$'s in the denominators of the propagators. These are necessary in order to take into account the time-ordering boundary condition.

Using that $\gamma^\mu\gamma^\alpha\gamma_\mu = -\gamma^\alpha$ and introducing usual Feynman parameters and using dimensional regularization, together with standard techniques, one finds

$$\Sigma_1(k,x') = \frac{e^2\not{k}}{16\pi^2}\int_0^1 du\sqrt{1-u}\left[\frac{1}{\bar{\epsilon}_\gamma} - \ln\left(\frac{\Delta - i\epsilon}{\mu^2}\right)\right] \tag{35}$$

where $\Delta = \Delta(u) = uM_e^2 + (1-u)M_\gamma^2 - u(1-u)k^2$ and

$$\frac{1}{\bar{\epsilon}_\gamma} \equiv \frac{1}{\epsilon_\gamma} - \gamma_E + \ln 4\pi, \tag{36}$$

γ_E is Euler's constant and as asserted above $2\epsilon_\gamma = 3 - d_e$.

Now let us present an explicit expression for the renormalization constant Z_2. Consider Eq. (31). Let us employ Riemann normal coordinates with origin at x'. In general, the expansions for $S_0(x,z)$ and $\Sigma_1(z,z')$ will be different from the expressions given previously since it is x' that is fixed and the arguments of such quantities do not contain x'. Then one should consider for $S_0(x,z)$ and $\Sigma_1(z,z')$ a more general momentum-space representation [48]. Nevertheless, at leading order the results are the same. Therefore, one finds the following one-loop local-momentum representation at leading order in the expansion in curvatures

$$S(k,x') = S_0(k,x') + S_0(k,x')\Sigma_1(k,x')S_0(k,x'). \tag{37}$$

Now consider the leading term in the expansion of $S_0(k,x')$. Since curvature effects are supposed to be sufficiently small, this can also be written as

$$S_{0,\text{leading}}(k,x') = \frac{\gamma^\nu k_\nu}{k^2 - M_e^2} = \frac{\gamma^\nu k_\nu}{k^2} + \frac{\gamma^\nu k_\nu}{k^4}\frac{R(x')}{12} + \cdots \tag{38}$$

in other words, we obtain the standard local-momentum representation. Hence Eq. (37) can be written as

$$iS(k,x') = \frac{i}{\not{k}} + \frac{i}{\not{k}}[-i\Sigma_1(k,x')]\frac{i}{\not{k}} + \cdots \tag{39}$$

where we are focusing only on the first term in the expansion for S_0 since this is the one important in discussing the

renormalization. On the other hand, since $\psi = Z_2^{1/2}\psi_R$, one obtains that $S = Z_2 S_R$. Hence following standard renormalization procedures, one finds that

$$Z_2 = 1 + \frac{2}{3}\frac{\alpha_R}{4\pi\bar{\epsilon}_\gamma} + \mathcal{O}(\alpha^2) \tag{40}$$

where we have replaced α by α_R in such an expression (this is correct to leading order). This has the same form as in flat space [27]. Observe also that renormalization constant Z_2 at one-loop is unaffected by space-time curvature, a result similar to the standard quantum electrodynamics in curved space-time [42]. Curvature terms only contribute to the finite part of the self-energy:

$$\begin{aligned}\Sigma_{1\mathrm{F}}(k,x') &= -\frac{e^2\not{k}}{16\pi^2}\int_0^1 du\sqrt{1-u}\ln\left(\frac{\Delta - i\epsilon}{\mu^2}\right)\\ &= -\frac{e^2\not{k}}{16\pi^2}\int_0^1 du\sqrt{u}\\ &\quad\times\ln\left(\frac{(1-u)M_e^2 + uM_\gamma^2 - i\epsilon - u(1-u)k^2}{\mu^2}\right).\end{aligned} \tag{41}$$

B. One-loop vertex correction

Let us now we turn our attentions to the vertex correction at one-loop order. This is given by the third expression in Eq. (30), see Fig. 2. Again considering Riemann normal coordinates with origin at x', one must insert into such an expression the field propagators calculated in the appendixes. By taking into account only the leading-order term of such an expansion, one finds that

$$\begin{aligned}e\Gamma_1^\mu(k_1,k_2,x') &= \frac{1}{2}\int\frac{d^3q}{(2\pi)^3}\frac{i\eta_{\alpha\beta}}{(q^2 - M_\gamma^2 + i\epsilon)^{1/2}}(-ie\gamma^\beta)\\ &\quad\times\frac{i(\not{k}_1 + \not{q})}{(k_1+q)^2 - M_e^2 + i\epsilon}(-ie\gamma^\mu)\\ &\quad\times\frac{i(\not{k}_2 + \not{q})}{(k_2+q)^2 - M_e^2 + i\epsilon}(-ie\gamma^\alpha)\end{aligned} \tag{42}$$

where as above we have considered the reduced gauge propagator in the Feynman gauge. After introducing suitable Feynman parameters and a simple change of variables, one finds that only one of the possible terms in the numerator produces an UV divergence—this is the one independent of k_1 and k_2. Physically we interpret it as a contribution to the charge form factor. So let us calculate the vertex function for $k_1 = k_2 = 0$. Again following the standard procedure, one finds

$$\begin{aligned}\tilde{\Gamma}_1^\mu(x') &= \frac{e^2}{32\pi^2}\int_0^1 dydz\frac{\theta(-y-z+1)\theta(y+z)}{\sqrt{1-y-z}}\\ &\quad\times\left[\frac{1}{\bar{\epsilon}_\gamma} - \frac{2}{3} - \ln\left(\frac{\tilde{\Delta}(y,z;0,0) - i\epsilon}{\tilde{\mu}^2}\right)\right]\gamma^\mu\end{aligned} \tag{43}$$

where

$$\begin{aligned}\tilde{\Delta}(y,z;k_1,k_2) &= (1-y-z)M_\gamma^2 + (y+z)M_e^2\\ &\quad + (yk_1 + zk_2)^2 - yk_1^2 - zk_2^2.\end{aligned}$$

Now we must discuss the one-loop renormalization of the vertex function. This amounts to calculate the renormalization constant Z_1 at one-loop level. Proceeding as in the previous section, the vertex function up to one-loop level in the local-momentum representation can be written as

$$-ie\Gamma^\mu(k_1,k_2,x') = -ie\gamma^\mu - ie\Gamma_1^\mu(k_1,k_2,x') \tag{44}$$

where as above we considered only the leading order in the expansion in curvatures. On the other hand, the renormalized vertex function Γ_R^μ is given in terms of the associated bare quantity Γ^μ and Z_1 as

$$\Gamma_R^\mu(k_1,k_2,x') = Z_1^{-1}\Gamma^\mu(k_1,k_2,x') \tag{45}$$

again in leading order in the expansion in curvatures. By using again the standard approach, one finds that

$$Z_1 = 1 + \frac{2}{3}\frac{\alpha_R}{4\pi\bar{\epsilon}_\gamma} + \mathcal{O}(\alpha^2). \tag{46}$$

where as above we have replaced α by α_R. A simple comparison between Eqs. (46) and (40) shows that $Z_1 = Z_2$. So we have explicitly verified the constraint between such renormalization constants at one-loop order: This result, which is a consequence of the Ward-Takahashi identity, is still valid for the curved-space version of RQED.

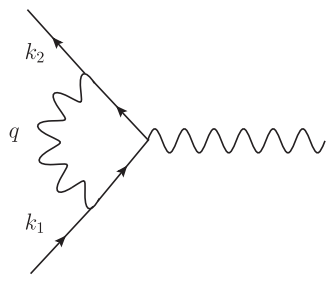

FIG. 2. One-loop vertex correction.

C. One-loop vacuum polarization

Finally let us discuss the one-loop vacuum polarization. This is given by the first expression in Eq. (30). See also Fig. 3. We will consider this calculation with more detail since we wish to explicitly check the aforementioned expectation concerning the vanishing of the one-loop beta function. Even though this is a somewhat standard calculation, we will give a step-by-step analysis of this issue, so

that our conclusions are presented in a clear way. The same goes for checking the Ward identity.

Again considering Riemann normal coordinates with origin at x', one must insert into such an expression the fermion propagator calculated in the Appendix B. By taking into account only the leading-order term of such an expansion, one finds that

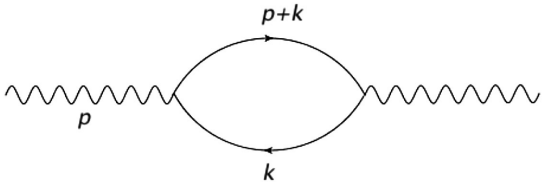

FIG. 3. One-loop vacuum polarization.

$$i\Pi_1^{\mu\nu}(p,x') = -e^2 \int \frac{d^3k}{(2\pi)^3} \mathrm{tr}[\gamma^\mu \gamma^\alpha \gamma^\nu \gamma^\beta] \frac{(p+k)_\alpha k_\beta}{((p+k)^2 - M_e^2 + i\epsilon)(k^2 - M_e^2 + i\epsilon)}. \tag{47}$$

As above, in such an equation use is made of the flat-space version of the gamma matrices. Using properties of the traces of products of gamma matrices and introducing Feynman parameters, one finds

$$i\Pi_1^{\mu\nu}(p,x') = -2e^2 \int_0^1 dx \int \frac{d^3k}{(2\pi)^3} \frac{((1-x)p+k)^\mu (k-xp)^\nu + \mu \leftrightarrow \nu - ((1-x)p+k).(k-xp)\eta^{\mu\nu}}{(k^2 - \bar{\Delta} + i\epsilon)^2}, \tag{48}$$

where $\bar{\Delta} = M_e^2 - x(1-x)p^2$ and we have redefined $k \to k - xp$. Keeping only even terms in k and considering that $k^\mu k^\nu \to k^2 \eta^{\mu\nu}/3$ inside the integral, we get

$$i\Pi_1^{\mu\nu}(p,x') = 2e^2 \int_0^1 dx \int \frac{d^3k}{(2\pi)^3} \frac{1}{(k^2 - \bar{\Delta} + i\epsilon)^2} \left[\left(\frac{1}{3} k^2 - x(1-x)p^2 \right) \eta^{\mu\nu} + 2x(1-x) p^\mu p^\nu \right]. \tag{49}$$

This contribution turns out to be finite. Using standard techniques to calculate the momentum integral, one obtains

$$i\Pi_1^{\mu\nu}(p,x') = -\frac{ie^2}{2\pi}(p^2\eta^{\mu\nu} - p^\mu p^\nu) \int_0^1 dx \frac{x(1-x)}{\sqrt{M_e^2 - i\epsilon - x(1-x)p^2}} + \frac{ie^2 M_e^2}{4\pi} \eta^{\mu\nu} \int_0^1 dx \frac{1}{\sqrt{M_e^2 - i\epsilon - x(1-x)p^2}}. \tag{50}$$

Apparently the Ward identity is violated by the presence of an anomalous contribution, given by the second term on the right-hand side of the above equation. However, by evaluating the x-integrals one finds that the transversality breaking term is actually longitudinal; more importantly, since the numerator is proportional to $M_e^2 = R(x')/12$, such a term is of higher order in the curvature expansion currently considered. Hence at leading order

$$i\Pi_1^{\mu\nu}(p,x') = \frac{ie^2}{4\pi}(p^2\eta^{\mu\nu} - p^\mu p^\nu) \left[\frac{\sqrt{M_e^2 - i\epsilon}}{p^2} + \frac{1}{4p} \ln \left(\frac{2\sqrt{M_e^2 - i\epsilon} - p}{2\sqrt{M_e^2 - i\epsilon} + p} \right) \right] \tag{51}$$

and the Ward identity at one-loop order is satisfied.

The most relevant upshot from this calculation is that the vacuum polarization is finite, at least at one-loop order. This means that such a contribution does not get renormalized, $\delta Z_3^{(1)} = 0$. This in turn implies that the beta function of the curved-space version of RQED is zero at one-loop order.

V. APPLICATION TO CURVED GRAPHENE LAYER

As described in [21] positive or negative intrinsic curvature in graphene arises by removing or introducing sites in a given hexagonal lattice ring. These are the so-called disclination defects. Dislocation defects (pair of disclinations of opposite curvature) introduce torsion but have zero net curvature [49–51]. Ripples due to thermal fluctuations have also been observed [52]. In this section we describe how to apply the formalism developed so far to the case of curved graphene layers.

An idealized model of a disclination in an elastic media is obtained when the curvature is concentrated at the tip of a cone. In this case, the geometry can be described by a metric similar to the one found in the discussions of a single cosmic string [18,53]. As well known, this generates a conical singularity in the curvature: The scalar curvature in this space will be proportional to a delta function [54,55]. Hence it appears at first sight that disclinations cannot be encompassed in the present formalism. However, an important issue concerns the core region of the defect. Indeed, realistic models of cosmic strings, in which the space-time curvature is spread over a region of finite size,

was discussed in detail in Ref. [56]. The main idea essentially consists in replacing the conical singularity by a smooth spherical cap. In such cosmological models the curvature is confined inside a cylinder, describing the interior structure of the string. Concerning a graphene sheet, the generation of a disclination by employing the usual "cut and glue" procedure will result in a true cone. This corresponds to a pointlike disclination defect and, in particular, implies the presence of a conical singularity. Notwithstanding, one must bear in mind that a membrane possesses finite elasticity, so a realistic situation must naturally go beyond the infinite-rigidity approximation. Thus, in order to have the curvature spread over some finite region one needs to take into account elastic properties. In other words, one needs to consider the graphene layer at finite elasticity [57,58]. For similar intriguing discussions regarding a realistic account of a physical lattice in graphene-like systems, see also Refs. [59,60]. In summary, a realistic picture of disclinations should take into account the finite elasticity of the graphene layer, and this amounts to considering a suitable procedure of regularization for the conical singularity (for interesting discussions regarding techniques for regularizing the conical singularity, see Refs. [61,62]). In such a situation, our formalism is expected to be fully operational and to provide sensible physical results. Other possible situations to which our formalism can be applied are those discussed in Ref. [15], where a quantum field theory in curved graphene was constructed. On the other hand, as well known it is possible to consider curved space-times with conical singularities but with well-behaved scalar curvatures [63]. In any case, around the tip of a cone (including the tip) a smooth differentiable structure is available. Indeed, a heat kernel expansion on spaces with a conical singularity can be derived [62,64,65], which implies that the local-momentum representation can also be used in such contexts.

There are two small modifications to be made. First of all photons, contrary to electrons, are not subjected to a curved space. Therefore we set $M_\gamma^2 = 0$. Notice however that the one-loop vacuum polarization (51) is not affected by M_γ^2 as there are no internal gauge field propagators. Importantly the Ward identity still holds for $M_\gamma^2 = 0$ as only a few immaterial factors of $|g|^{1/2}$ drop out. This is confirmed by the recovery of the known UV divergences from flat graphene, see from [66].

In turn, we must substitute γ^i by $v_F\gamma^i$, with $v_F \approx 1/300$. This takes into account the actual Fermi velocity of the Dirac excitations. The system (32) of renormalized parameters is then complemented by

$$v_F = Z_v v_R. \tag{52}$$

It has been shown that the relativistic theory with $v_F = c = 1$ is a fixed point in the infrared [37,66]. It must be kept in mind that v, hence also Z_v, enter only alongside the spatial components of the gamma matrices. This results in a slightly more involved renormalization procedure as the frequency parts of both the fermion self-energy and vertex correction are proportional to Z_2 and Z_1, whereas the momentum parts are proportional to $Z_2 Z_v$ and $Z_1 Z_v$. By virtue of the Ward Identity $Z_1 = Z_2$ it is seen that the fermion wave function and vertex renormalize equally as usual. This suggests two independent ways to compute Z_v, the simplest being through the fermion self-energy.

The Feynman rules for the application of the theory to graphene for the case of retarded Coulomb interaction produce the following expressions for the fermionic and gauge-field propagator, and the photon-fermion-fermion vertex, respectively:

$$\begin{aligned} iS_0(\omega_p, \mathbf{p}) &= \frac{i(\gamma^0\omega_p - v_F\gamma^i p^i)}{\omega_p^2 - v_F^2\mathbf{p}^2 - M_e^2 v_F^4} \\ iD_0(\omega_p, \mathbf{p}) &= \frac{1}{2}\frac{i}{\sqrt{-\omega_p^2 + \mathbf{p}^2}} \\ -ie\Gamma_0^0 &= -ie\gamma^0. \end{aligned} \tag{53}$$

The free fermion propagator above has the feature that it does not modify the density of states at x' because $M_e^2(x')$ is a momentum-independent constant within our framework. This readily follows from

$$\rho(\omega) = -\frac{1}{\pi}\mathrm{Im}\int d^2\mathbf{k}\,\mathrm{Tr}\left[\frac{\gamma^0\omega - v_F\boldsymbol{\gamma}.\mathbf{k}}{\omega^2 - v_F^2\mathbf{k}^2 - M_e^2 v_F^4}\gamma^0\right], \tag{54}$$

by use of the standard identity for the principal value P

$$P\left(\frac{1}{x \pm i\epsilon}\right) = \frac{1}{x} \mp i\pi\delta(x). \tag{55}$$

Performing the integral with polar coordinates the Jacobian factor of k cancels with one arising from the delta function $\delta(\omega^2 - v_F^2 k^2 - M_e^2 v_F^4)$, leading to the usual linear ω/v_F^2 behavior around the Dirac points.

A. 1-loop fermion self-energy

Let us discuss the one-loop self-energy. One finds that

$$-i\Sigma_1(\omega_p, \mathbf{p}) = \frac{e^2}{2}\int \frac{d^{d-1}\mathbf{k}}{(2\pi)^{d-1}}\frac{d\omega_k}{2\pi}\frac{\gamma^0(\gamma^0(\omega_k + \omega_p) - v_F\gamma^i(k+p)_i)\gamma^0}{((\omega_k + \omega_p)^2 - v_F^2(\mathbf{k}+\mathbf{p})^2 - M_e^2 v_F^4)(\omega_k^2 - \mathbf{k}^2)^{1/2}}. \tag{56}$$

Having already established that the UV divergences are in general the same as in the flat model, we just state the result for the Fermi-velocity renormalization

$$\delta Z_v = -\frac{\alpha_g}{4\pi}\left(\frac{3}{1-v_F^2} - \frac{(1+2v_F^2)\cos^{-1}v_F}{v_F(1-v_F^2)^{3/2}}\right). \quad (57)$$

which, apart from a constant factor proportional to the square of the Fermi velocity (coming from the current density interaction of the vertex we have dropped), recovers the results from Ref. [37], to which we refer the reader for a detailed computation. The Fermi velocity beta function β_v is shown in Fig. 4. The crucial point here is that, according to our model, the relativistic fixed point achieved for $v_F \to 1$ is predicted to survive in the presence of disclination-induced curvature. Here $\alpha_g = e^2/(4\pi v_F)$. As for the finite part of the self energy, we are particularly interested in the imaginary part of Σ_1^F as it translates to the scattering time among the charge carriers in graphene due to the electromagnetic interaction in the presence of curvature. The local $\mathbf{p} \to 0$ limit is relevant when considering level-broadening effects on the conductivity. Hence

$$\Sigma_1^F(\omega_p) = -\frac{\alpha_g}{4\pi}\gamma^0\omega_p \int_0^1 dx \frac{\sqrt{1-x}}{1-x(1-v_F^2)} \times \log\left(\frac{\bar{\mu}^2}{x(M_e^2 v_F^4 - (1-x)\omega_p^2) - i\epsilon}\right) \quad (58)$$

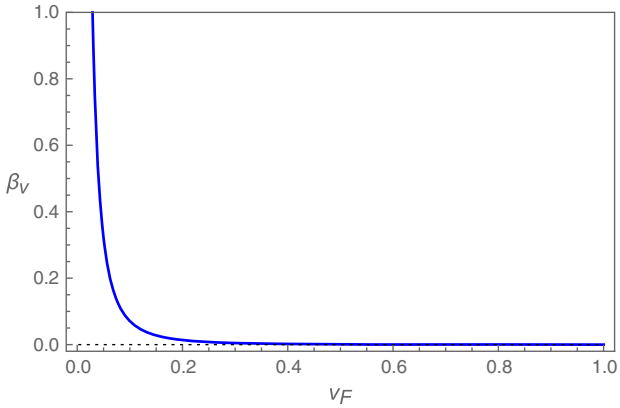

FIG. 4. Fermi velocity 1-loop beta function for graphene with retarded Coulomb interaction.

There are now two possible cases to consider, namely positive or negative Ricci scalar. For positive Ricci scalar, i.e., $M_e^2 > 0$, we obtain, for the scattering time:

$$\tau_+^{-1}(z) = \frac{\alpha_g}{4} M_e v_F^2 z \int_0^1 dx \frac{\sqrt{1-x}}{1-x(1-v_F^2)} \theta((1-x)z^2 - 1), \quad (59)$$

where $z^2 = \omega_p^2/M_e^2 v_F^4$. This integrates to

$$\tau_+^{-1}(z) = \begin{cases} 0, & z \le 1 \\ \frac{\alpha_g}{4} M_e v_F^2 z\left(\frac{2}{1-v_F^2}\left(1-\frac{1}{z}\right) + \frac{2}{(1-v_F^2)^{3/2}}\left(\cot^{-1}\left(\frac{v_F z}{\sqrt{1-v_F^2}}\right) - \cos^{-1}v_F\right)\right), & z > 1. \end{cases} \quad (60)$$

For negative Ricci scalar, i.e., $M_e^2 < 0$, the self-energy always acquires an imaginary part. In this case, the scattering time is given by

$$\tau_-^{-1}(z) = \frac{\alpha_g}{4} M_e v_F^2 z\left(\frac{2}{1-v_F^2} - \frac{2v_F\cos^{-1}v_F}{(1-v_F^2)^{3/2}}\right). \quad (61)$$

From the imaginary part of the self-energy, one can use standard dispersion relations to calculate the real part and, as a result, one is able to evaluate explicitly the quasiparticle residue at the Fermi energy. As will be argued in due course, the quantity $M_e v_F^2$ for positive Ricci scalar may play the role of an effective chemical potential. Using this as the value of the Fermi energy in the present context, one can easily show that the quasiparticle residue asymptotically should acquire a nonzero value at the Fermi energy in the case $M_e^2 > 0$. All such results concerning the self-energy should be compared with the ones of Refs. [66,67].

B. 1-loop vertex correction

Now let us consider the one-loop vertex correction at zero external momenta. This is given by

$$-ie\Gamma_1^\mu(0,0) = \frac{e^3}{2}\int \frac{d^{d-1}\mathbf{k}}{(2\pi)^{d-1}}\frac{d\omega_k}{2\pi}\frac{\gamma^0\gamma^\alpha\gamma^\mu\gamma^\beta\gamma^0 k_\alpha k_\beta}{(\omega_k^2 - v_F^2\mathbf{k}^2)^2(-\omega_k^2+\mathbf{k}^2)^{1/2}}. \quad (62)$$

It is straightforward to check that the UV divergences match those of $-i\Sigma_1$. We once more refer to Ref. [37] for the details. The finite parts of the time and spatial components read

$$\Gamma_1^{0,F}\gamma^0 = -\frac{\alpha\gamma^0}{8\pi}\int_0^1 dx\frac{x}{\sqrt{1-x}}\left(\frac{1}{1-x(1-v_F^2)}-\frac{2v_F^2}{(1-x(1-v_F^2))^2}\right)\log\left(\frac{(1-x(1-v_F^2))\bar{\mu}^2}{xM_e^2v_F^4}\right), \tag{63}$$

and

$$v_F\Gamma_1^{i,F}\gamma^i = -\frac{\alpha v_F\gamma^i}{8\pi}\int_0^1 dx\frac{x}{\sqrt{1-x}}\left(\frac{1}{1-x(1-v_F^2)}\log\left(\frac{(1-x(1-v_F^2))\bar{\mu}^2}{xM_e^2v_F^4}\right)+\frac{v_F^2}{(1-x(1-v_F^2)^2}\right). \tag{64}$$

These allow us to define a suitable effective Fermi velocity:

$$\frac{1}{v_{\text{eff}}} = \frac{1}{v_F}\left(1+\frac{(\Gamma_1^{0,F})^3}{\Gamma_1^{i,F}}\right). \tag{65}$$

At the point $\bar{\mu}^2 = M_e^2v_F^4$ the correction leads to a higher effective Fermi velocity in accordance with expectation from the running in Fig. 4

$$v_{\text{eff}} \approx 1.0072 v_F. \tag{66}$$

In Ref. [17] it was shown that the effect of curvature on the electronic properties of a graphene sheet leads to a decrease in the Fermi velocity in comparison with the free velocity. On the other hand, electron-electron interactions tend to increase the Fermi velocity. In our model, we see that both effects seem to be important, and their combination contribute decisively to a slight increase in v_F. We remark that this conclusion was obtained for the choice $\bar{\mu}^2 = M_e^2v_F^4$, so one must be very careful with possibly naive physical interpretations. In particular, this shows once more the importance of considering a finite elasticity for the graphene layer—for ideal disclinations, M_e^2 would present a sharp singular behavior, as discussed above, and this choice as a renormalization point would become problematic. A renormalization-group treatment would be most welcome here. This would indeed be interesting to explore, and we hope to consider this calculation in the future.

C. Higher-frequency behavior of the optical conductivity

As an application of the above results, let us determine the high-frequency behavior of the optical conductivity in the presence of curvature effects in graphene by using the Kubo formula, which describes the linear response to a static external electric field. In real time, it is given by

$$\sigma^{ik} = \lim_{\mathbf{p}\to 0} i\frac{\langle j^i j^k\rangle}{\omega+i\epsilon} \tag{67}$$

where the current correlation function is meant to contain only one-particle irreducible (1PI) diagrams. A simple analysis shows that [26]

$$\langle j_\mu j_\nu\rangle_{1\text{PI}} = \Pi_{\mu\nu} \tag{68}$$

where $\Pi_{\mu\nu}$ is the vacuum polarization tensor of the electromagnetic field. The optical conductivity is then given by

$$\sigma^{jk}(\omega) = \lim_{\mathbf{p}\to 0}\frac{i\Pi^{jk}}{\omega+i\epsilon}. \tag{69}$$

To derive the optical conductivity from the above formula, one must change the boundary conditions employed so far. This amounts to considering the various Green functions appearing in Eq. (30) with retarded boundary conditions. In this case the loop integrals in the vacuum polarization are to be calculated using the in-in formalism, see for instance Ref. [68]. The result has the same functional dependence, but with a different $i\epsilon$ prescription:

$$q^0 \to q^0 + i\epsilon.$$

The one-loop vacuum polarization is then given by

$$\begin{aligned} i\Pi_1^{\mu\nu}(p,x') &= \frac{ie^2}{4\pi}(p^2\eta^{\mu\nu}-p^\mu p^\nu) \\ &\quad\times\left[\frac{\sqrt{M_e^2v_F^4}}{p^2}+\frac{1}{4p}\ln\left(\frac{2\sqrt{M_e^2v_F^4}-p}{2\sqrt{M_e^2v_F^4}+p}\right)\right], \\ p^\mu &= (p^0+i\epsilon,\mathbf{p}). \end{aligned} \tag{70}$$

Geometrically it is perfectly plausible for M_e^2 to be either negative or positive. Both possibilities seem to lead to qualitatively different behavior due to extra factors of i arising for $M_e^2<0$. In the following we will focus mostly on the positive scalar-curvature case where the physics is clearer, and we give only a brief discussion on the negative case at the end of this section. With that in mind, we combine our results to obtain the high-frequency behavior of the optical conductivity:

$$\sigma^{jk}(z,x') = \frac{e^2}{4}\left[\frac{4}{\pi}\frac{i}{z+i\epsilon}+1+\frac{i}{\pi}\ln\left(\frac{z+i\epsilon-2}{z+i\epsilon+2}\right)\right]\eta^{jk}. \tag{71}$$

Observe that σ^{jk} a function of the ratio $z=\omega/\sqrt{M_e^2v_F^4}$. The real and imaginary parts of σ^{jk} are given by, for $z\neq 0$:

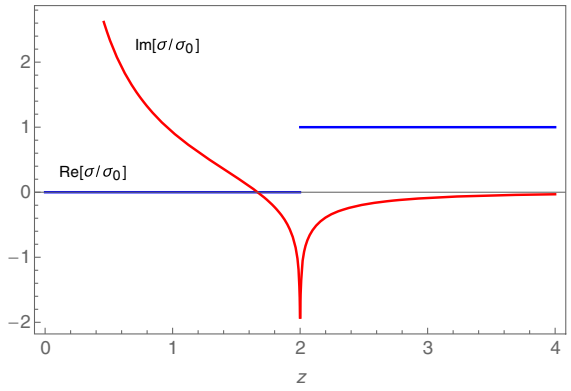

(a) Real and imaginary parts of $\sigma^{jj}(z,x')$ normalized to σ_0 without broadening effects.

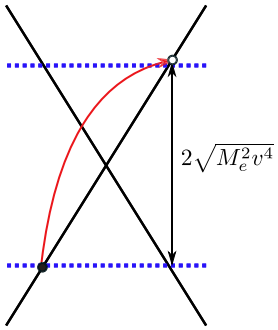

(b) Origin of conductivity jump under a finite chemical potential (blue line).

FIG. 5. Noninteracting conductivity in graphene with a finite chemical potential.

$$\mathrm{Re}[\sigma^{jk}(z,x')] = \frac{e^2}{4}\theta(z-2)\eta^{jk}$$
$$\mathrm{Im}[\sigma^{jk}(z,x')] = \frac{e^2}{4\pi}\left(\frac{4}{z} - \ln\left|\frac{z+2}{z-2}\right|\right)\eta^{jk}. \quad (72)$$

The conductivity for the case $M_e^2 > 0$ is depicted in Fig. 5(a). In this way, we recover the results presented in Refs. [69,70] for zero temperature and zero mass gap, but finite chemical potential in the local limit. Remarkably, such equations also show that $\sqrt{M_e^2 v_F^4}$ cannot play the role of a mass gap in the expression for the optical conductivity. Rather, our results, combined with those obtained in Refs. [69,70], seem to suggest an effective chemical-potential interpretation for $\sqrt{M_e^2 v_F^4}$, at least as far as the optical conductivity is concerned. At the moment we do not have more elements to argue in favor of the general validity of this interpretation. In any case, this allows us to understand the first term in Eq. (71) as due to intraband transitions, and the remaining as the interband contribution. The latter is just the minimal graphene conductivity $\sigma_0 = e^2/4$ for $z > 2$. The absence of interband transitions for $z < 2$ is due to the kinematics of momentum conservation of chiral fermions as illustrated in Fig. 5(b). Even though the validity of the local momentum representation translates to high-frequency regime, our result seems to work for all z given the identification $\sqrt{M_e^2 v_F^4} = \mu$.

If one wishes to include curvature effects of level broadening due to scattering of the fermion, then one should replace $i\epsilon$ by $\tau_+^{-1}(z)$ in the expression of the optical conductivity. One obtains

$$\sigma^{jk}(z,x') = \frac{e^2}{4}\left[\frac{4}{\pi}\frac{i}{z + i\tau_+^{-1}(z)} + 1 + \frac{i}{\pi}\ln\left(\frac{z + i\tau_+^{-1}(z) - 2}{z + i\tau_+^{-1}(z) + 2}\right)\right]\eta^{jk}. \quad (73)$$

If $\mathrm{Im}[\Sigma_1^F(\omega)]$ is small, we can approximate it as a constant value, which results in a constant τ_+^{-1}. This implies that in this case this expression can also be obtained by employing resummed fermionic propagators in the calculation of the vacuum polarization. The result will resemble a simple one-loop calculation, even though higher-order corrections are being taken into account with the usage of dressed propagators. This is somewhat reminiscent of the standard discussion on unstable particles in high-energy scattering amplitudes within the narrow-width approximation. In the context of condensed-matter settings, a vanishingly small imaginary part of the self-energy (around the Fermi surface) implies that the criterion for the Fermi-Landau liquid theory is fully justified.

Let us first consider the full frequency dependence of τ_+^{-1}. When $M_e^2 > 0$ we see from Fig. 6 that there is no longer a jump on the real part of the conductivity at $z = 2$. Instead, the conductivity starts to increase smoothly at $z = 1$. Accordingly the imaginary part of $\sigma(z)$ is also smoothed at $z = 2$, as dictated by the Kramers-Kronig relations. For $z \to \infty$ we still recover σ_0. Eq. (73) is similar

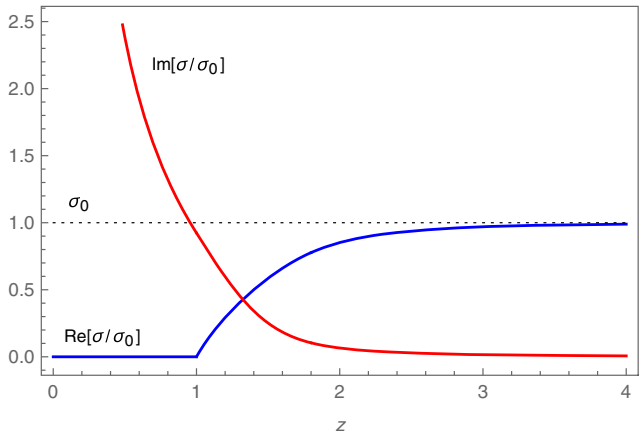

FIG. 6. Real and imaginary parts of optical conductivity normalized to σ_0 with broadening effects for positive Ricci curvature scalar. Dotted line shows that the minimum conductivity σ_0 is approached asymptotically.

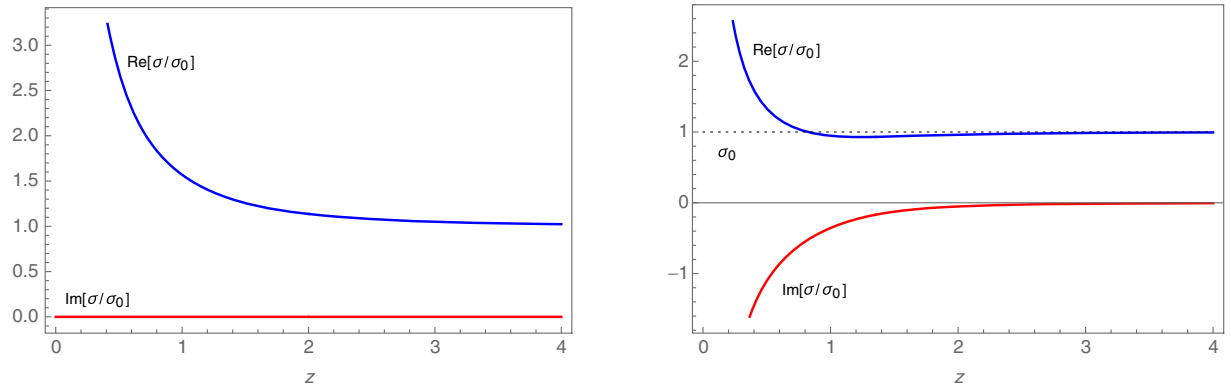

(a) Real and imaginary parts of non-interacting optical conductivity normalized to σ_0.

(b) Real and imaginary parts of optical conductivity normalized to σ_0 with broadening effects.

FIG. 7. Conductivity in graphene for negative Ricci scalar.

to the one found in Ref. [71], except for the fact that here the scattering time given by Eq. (60) kicks in only at $z = 1$. Indeed, these authors considered $\tau_+^{-1}(z)$ at $z = 1$ in the first term and $\tau_+^{-1}(z) \to \tau_+^{-1}(z/2)$ in the logarithmic term (in our notation) whereas we have considered the full frequency dependence of τ_+^{-1}. The reason for this difference in the approaches lies in the fact that the energy dependence of the scattering time in both models behave differently at the Fermi energy, as just mentioned, since they describe different physical situations. Nevertheless, as shown by these authors, the scaling of the dynamical conductivity leads to a singular jump at $\omega = 0$ for zero Fermi energy, a result that clearly resembles the behavior of $\mathrm{Im}[\sigma]$ in our model.

One may consider the conductivity for a fixed value of τ_+^{-1}, somewhat partially similar to what was undertaken in Ref. [71]. We explore this situation for the case in which $\mathrm{Im}[\Sigma_1^F(\omega)]$ is small so that τ_+^{-1} can be taken to be approximately constant. This will take place near the Fermi energy. As an illustration, let us quote our result for a matching scale of $z = z_0$, $z_0 \gtrsim 1$, for the scattering time (Fermi energy amounts to choosing $z_0 = 1$):

$$\sigma^{jk}(z,x') = \frac{e^2}{4}\left[\frac{4}{\pi}\frac{i}{z+i\tau_+^{-1}(z_0)} + 1 + \frac{i}{\pi}\ln\left(\frac{z+i\tau_+^{-1}(z_0)-2}{z+i\tau_+^{-1}(z_0)+2}\right)\right]\eta^{jk}. \quad (74)$$

It is easy to see that there is an enhancement in the conductivity for $z \geq 2$:

$$\sigma_0 \to \sigma_0 + \frac{e^2}{\pi}\frac{\tau_+^{-1}(z_0)}{z^2+\tau_+^{-2}(z_0)}. \quad (75)$$

For $z < 2$ the intraband contribution produces a positive contribution to the real part of the optical conductivity, whereas the log yields a (constant) negative contribution. However, for $z \to 0$, the intraband transition is the dominant term, and a positive contribution remains. In order to confirm this analysis we would have to calculate the optical conductivity for all regimes of frequency which would mean going beyond the large-momentum expansion used above for the propagators. We do not have a clear evaluation of this physics, but at least the conclusion seems indeed to be that curvature effects should contribute positively to the conductivity of graphene. This is in accordance with the arguments and expectations of Ref. [26].

Let us now turn our attentions to the $M_e^2 < 0$ case. The optical conductivity reads now

$$\sigma^{jk}(z,x') = \frac{e^2}{2}\left[\frac{4}{\pi}\frac{1}{z+i\tau_-^{-1}(z)} + 1 + \frac{i}{\pi}\ln\left(\frac{z+i\tau_-^{-1}+2i}{z+i\tau_-^{-1}-2i}\right)\right]. \quad (76)$$

Figure 7(a) describes the noninteracting optical conductivity ($\tau_-^{-1} = 0$ above). Here the model seems to run into trouble with the Kramers-Kronig relations as pointed out by the vanishing of the imaginary component. In comparison with Eq. (71), we note the source of its imaginary component is solely due to the first term, i.e., the intraband transitions. For $M_e^2 < 0$ (and $\tau_-^{-1} = 0$) this term becomes purely real. Inclusion of broadening effects seems to lift the problem as shown in Fig. 7(b). Here the real component also assumes a form similar to Ref. [71] although it always stays very close to σ_0 after it crosses it from the above.

VI. CONCLUSIONS

The primary aim of this work was to develop a formalism to study the curved-space RQED by employing the local momentum representation. Then we applied the model, with slight modifications, to graphene. In particular the optical conductivity was computed to one-loop and at leading adiabatic order surprisingly revealing the

appearance of an effective chemical potential for the positive Ricci scalar case. Importantly, this effect is nonperturbative as it stems from the partial ressumation of the Ricci scalar. Furthermore, we demonstrated how the combined effect of intrinsic curvature of the graphene sheet and electron-electron interactions as described by the curved-space RQED could affect the optical conductivity. In summary, by comparing the outcomes of the present paper with the ones in the existing literature, we have showed that the curved-space RQED as a model for describing transport properties of curved graphene layers is able to (re)produce sensible physical results.

There are many open questions outside our scope that are nonetheless of great importance. Most obvious is developing curved space RQED beyond the approximations presented here. Within our approach it would also be interesting to study the trace anomaly and conformal invariance of the model. Research into possible holographic models (both for flat and curved RQED) would be most welcome for providing a tool into the nonperturbative regime. A two-loop analysis is also desirable specially for a more rigorous account of electron-electron interaction contributions to the optical conductivity. Additionally a computation of the global conductivity $\sigma(\omega)$ from the local $\sigma(\omega, x')$ by a disorder averaging treatment of $M_e^2(x')$ is expected to accurately model real samples. On the other hand, a nontrivial interesting generalization of our work could include torsion [72,73]. We hope to access these issues in future works.

ACKNOWLEDGMENTS

We thank T. Micklitz for invaluable discussions, in particular for bringing to our attention the possibility of applying techniques from quantum field theory in curved space in approaching the problem of the optical conductivity in graphene. We also thank A. Iorio and P. Pais for useful comments and discussions. The work of GM has been partially supported by Conselho Nacional de Desenvolvimento Científico e Tecnológico—CNPq under Grant No. 310291/2018-6, and Fundação Carlos Chagas Filho de Amparo à Pesquisa do Estado do Rio de Janeiro—FAPERJ under Grant No. E-26/202.725/2018.

APPENDIX A: RIEMANN NORMAL COORDINATES EXPANSION

The construction of Riemann normal coordinates about some point x' in the manifold goes as follows. On x' it is possible to make $g_{\mu\nu}(x') = \eta_{\mu\nu}(x')$ along with $\Gamma^{\alpha}{}_{\mu\nu}(x') = 0$. Now suppose that points x in the neighborhood of x' can be reached by a unique geodesic starting from x'. This is the so-called normal neighborhood of x'. We can make use of the tangent vectors to the geodesics to introduce a normal coordinate system X^{μ} with origin at x' such that

$$\frac{d^2X^{\alpha}}{d\lambda^2} = 0 \tag{A1}$$

along any geodesic, with λ some affine parameter describing the geodesic. By expanding with respect to these coordinates one finds that [46,74]

$$\begin{aligned} g_{\mu\nu}(x) &= \eta_{\mu\nu} - \frac{1}{3}R_{\mu\rho\sigma\nu}(x')X^{\rho}X^{\sigma} + \cdots \\ (-g(x))^{1/2} &= 1 + \frac{1}{6}R_{\mu\nu}(x')X^{\mu}X^{\nu} + \cdots \\ \Gamma_{\mu}{}^{i}{}_{j}(x) &= -\frac{1}{4}R_{\mu\rho ab}(x')(J^{ab})^{i}_{j}X^{\rho} + \cdots \\ Q^{i}{}_{j}(x) &= Q^{i}{}_{j}(x') + \cdots \\ e_a{}^{\mu}(x) &= e_a{}^{\nu}(x')\left(\delta^{\mu}_{\nu} + \frac{1}{6}R_{\nu\alpha}{}^{\mu}{}_{\beta}(x')X^{\alpha}X^{\beta}\right) + \cdots \end{aligned} \tag{A2}$$

where only the lowest-order terms are retained. Here $R_{\mu\rho ab}$ is the Riemann curvature tensor with two vielbein indices and J^{ab} is the Lorentz generator for the representation appropriate to the field under consideration. Also $Q^{i}{}_{j}$ is a quantity proportional to the curvature. Let us derive the expansion for the spin connection. From Eq. (A2), one finds

$$\omega_{\mu ab} = -\frac{1}{2}R_{\mu\rho ab}(x')X^{\rho} \tag{A3}$$

where we used the cyclicity property of the Riemann tensor. Hence

$$\begin{aligned} \Omega_{\mu} &= \frac{1}{2}\omega_{\mu ab}J^{ab} = -\frac{1}{4}R_{\mu\rho ab}(x')X^{\rho}J^{ab} \\ &= -\frac{1}{8}R_{\mu\rho ab}(x')\gamma^{a}\gamma^{b}X^{\rho} \end{aligned} \tag{A4}$$

which implies that

$$\begin{aligned} \gamma^{\mu}(x)\nabla_{\mu} &= \gamma^{a}e_a{}^{\mu}(x)(\partial_{\mu} + \Omega_{\mu}) \\ &= \gamma^{\nu}(x')\left(\partial_{\nu} + \frac{1}{6}R^{\mu}{}_{\alpha\nu\beta}(x')X^{\alpha}X^{\beta}\partial_{\mu}\right. \\ &\quad \left. - \frac{1}{8}R_{ab\nu\rho}(x')\gamma^{a}\gamma^{b}X^{\rho}\right). \end{aligned} \tag{A5}$$

However, using the anticommutation relations for the gamma matrices and again the cyclicity property of the Riemann tensor, one finds that

$$R_{abc\rho}\gamma^{c}\gamma^{a}\gamma^{b} = 2R_{a\rho}\gamma^{a}$$

which yields

$$\gamma^{\mu}(x)\nabla_{\mu}=\gamma^{\nu}(x')\left(\partial_{\nu}+\frac{1}{6}R^{\mu}{}_{\alpha\nu\beta}(x')X^{\alpha}X^{\beta}\partial_{\mu}-\frac{1}{4}R_{\nu\rho}(x')X^{\rho}\right). \tag{A6}$$

APPENDIX B: LOCAL-MOMENTUM REPRESENTATION OF THE FERMIONIC PROPAGATOR

In this Appendix we consider the local-momentum representation for the fermion propagator. The standard representation has been extensively discussed in the literature, see for instance Refs. [46,75,76]. Typically, since curvature effects are small, we will be interested only in the leading terms in the Riemann curvature. But for the moment we will keep our discussion as general as possible. In principle, we could follow the same steps outlined above. There is, however, another alternative form of proper-time expansion for propagators in curved spacetime which could be useful here. It is based on a partial resummation of the above series [77]. Consider Eq. (21) with $\vartheta=-1$. One can write the Green's function as

$$G(x,x')=-i\int_0^{\infty}ds\langle x,s|x',0\rangle \tag{B1}$$

where we omitted matrix indices, and the kernel $\langle x,s|x',0\rangle$ has a Schwinger-DeWitt expansion given by [78]

$$\begin{aligned}\langle x,s|x',0\rangle &= i(4\pi is)^{-d/2}e^{i\sigma(x,x')/2s}\Delta_{\mathrm{VM}}^{1/2}(x,x')F(x,x';is)\\ F(x,x';is) &= \mathbf{1}+\sum_{j=1}^{\infty}(is)^j f_j(x,x')\end{aligned} \tag{B2}$$

where $2\sigma(x,x')$ is the square of the proper arc length along the geodesic from x' to x and $\Delta_{\mathrm{VM}}(x,x')$ is the Van Vleck-Morette determinant defined by [79]

$$\Delta_{\mathrm{VM}}(x,x')=-|g(x)|^{-1/2}|g(x')|^{-1/2}\det\left[-\frac{\partial^2\sigma(x,x')}{\partial x^{\mu}\partial'^{\nu}}\right]. \tag{B3}$$

In turn, such an expansion can be rewritten in the form

$$\begin{aligned}\langle x,s|x',0\rangle &= i(4\pi is)^{-d/2}e^{i\sigma(x,x')/2s}\Delta_{\mathrm{VM}}^{1/2}(x,x')\bar{F}(x,x';is)\\ &\quad\times e^{-is[Q(x')-\frac{1}{6}R(x')]}\\ \bar{F}(x,x';is) &= \mathbf{1}+\sum_{j=1}^{\infty}(is)^j\bar{f}_j(x,x')\end{aligned} \tag{B4}$$

an assertion which was proved in Ref. [77]. The coefficients $\bar{f}_j(x,x')$ are R independent to all orders, but generically depend on the Ricci curvature and the Riemann tensor and their powers and derivatives. In addition, we stress that such coefficients in the fermionic case should be envisaged as bispinors; hence to perform properly the above expansion one should form the contraction between such bispinors with the bispinor of parallel displacement $\boldsymbol{\sigma}(x,x')$. It can be proved that $\boldsymbol{\sigma}(x,x')=\bar{f}_0(x,x')=\mathbf{1}$ [43].

The term $e^{-is[Q(x')-\frac{1}{6}R(x')\mathbf{1}]}$ should be defined as a a formal matrix power series ($\mathbf{1}$ is the unit spinor, in the case of fermions). A straightforward calculation yields

$$\begin{aligned}&\bar{F}(x,x';is)e^{-is[Q(x')-\frac{1}{6}R(x')\mathbf{1}]}\\ &\quad=\mathbf{1}+(is)(\bar{f}_1(x,x')-A(x'))\\ &\qquad+(is)^2\left(\bar{f}_2(x,x')+\frac{1}{2}A^2(x')-\bar{f}_1(x,x')A(x')\right)\\ &\qquad+\cdots\end{aligned} \tag{B5}$$

where $A(x')=Q(x')-R(x')/6$. Since such expansions should be equal, one finds that

$$\begin{aligned}\bar{f}_1(x,x') &= f_1(x,x')+A(x')\\ \bar{f}_2(x,x') &= f_2(x,x')-\frac{1}{2}A^2(x')+(f_1(x,x')+A(x'))A(x')\end{aligned} \tag{B6}$$

and so on. On the other hand, with Riemann normal coordinates y^{μ} for the point x with origin at the point x', one has that

$$f_1(x,x')=f_1(x')+f_{1\alpha}(x')y^{\alpha}+f_{1\alpha\beta}(x')y^{\alpha}y^{\beta}+\mathcal{O}(y^3)$$

where an expansion about the point x' was considered. The coefficients $f_{j\alpha\beta\ldots}$ are all proportional to derivatives of the f_j evaluated at the origin of the Riemann normal coordinates (i.e., at x'). The coefficients f_j have been calculated in the literature [43]. In particular, $\bar{f}_1=0$.

Now use the fact that, in Riemann normal coordinates about x', $\Delta_{\mathrm{VM}}(x,x')=|g(x)|^{-1/2}$, together with the results

$$\begin{aligned}&\int\frac{d^Dk}{(2\pi)^D}e^{-is(-k^2+m^2)-iky}\\ &\qquad=i(4\pi is)^{-d/2}e^{i\sigma(x,x')/2s}e^{-ism^2}\end{aligned} \tag{B7}$$

where $\sigma(x,x')=-y_{\alpha}y^{\alpha}/2$, and

$$\int_0^{\infty}ids e^{-is(-k^2+m^2)}=\frac{1}{-k^2+m^2}$$

to obtain that

$$G(x,x') = \Delta^{1/2}_{\rm VM}(x,x') \int \frac{d^D k}{(2\pi)^D} e^{-iky} \times \bar{F}\left(x,x';-\frac{\partial}{\partial m^2}\right)\frac{1}{k^2-m^2} \tag{B8}$$

where $m^2 = Q(x') - R(x')/6$ (Q now is just a function). Here $D = d_e$ for the case of the fermionic propagator. We also consider the replacement

$$y^\alpha \to i\frac{\partial}{\partial k_\alpha} \tag{B9}$$

in the above expression.

Now we are in the position of presenting an explicit expression for the fermionic propagator using Riemann normal coordinates about x'. Using that $m^2 = M_e^2 = R(x')/12$ for fermions as well as the above expansions for $\Delta_{\rm VM}(x,x')$ and $\gamma^\mu\nabla_\mu$, one finds, for the fermionic propagator

$$S_0(x,x') = \int \frac{d^D k}{(2\pi)^D} e^{-iky}\left[\frac{\gamma^\nu k_\nu}{k^2-M_e^2} + \frac{1}{(k^2-M_e^2)^2}\left(\frac{1}{2}R_{\nu\rho}\gamma^\nu k^\rho - \frac{\gamma^\nu k_\nu}{6}R\right) + \frac{2}{3}\frac{\gamma^\nu k_\nu k^\sigma k^\rho R_{\rho\sigma}}{(k^2-M_e^2)^3} + \cdots\right] \tag{B10}$$

where in the above equation γ^μ is the usual gamma matrix in flat space and $R = R_{\mu\nu}\eta^{\mu\nu}$ when considering only terms linear in the curvature for the expansion of $g^{\mu\nu}$ in Riemann normal coordinates.

APPENDIX C: LOCAL-MOMENTUM REPRESENTATION OF THE GAUGE PROPAGATOR

In this Appendix we present the local-momentum representation of the gauge propagator. For a standard discussion, see for instance Refs. [46,74,80]. In the present case, one has that the gauge propagator obeys Eq. (23). Following [77,81] one has, for the gauge propagator (in the Feynman gauge $\xi = 1$)

$$G^\mu{}_{\nu'}(x,x') = i\int_0^\infty ds \langle x,s|x',0\rangle^\mu{}_{\nu'} \tag{C1}$$

with

$$\langle x,s|x',0\rangle^\mu{}_{\nu'} = i(4\pi i s)^{-d/2} e^{i\sigma(x,x')/2s}\Delta^{1/2}_{\rm VM}(x,x') \times \bar{H}^\mu{}_{\nu'}(x,x';is)e^{isR(x')/6}$$

$$\bar{H}^\mu{}_{\nu'}(x,x';is) = g^\mu{}_{\nu'}(x,x') + \sum_{j=1}^\infty (is)^j \bar{h}_j{}^\mu{}_{\nu'}(x,x') \tag{C2}$$

We stress that $\bar{h}_j{}^\mu{}_{\nu'}$ is a bivector. Recall that, for a proper expansion of a bivector, such as the gauge propagator, one must form the combination $g^{\nu}{}_{\lambda'}G^{\mu\lambda'}$, which is a contravariant tensor of rank two at x and a scalar at x'. The object $g^{\nu}{}_{\lambda'}$ is the bivector of parallel transport from x' to x [82]. Note that $g_{\mu\nu'}(x,x) = g_{\mu\nu}$.

Proceeding with analogous considerations as above, one obtains that

$$\begin{aligned}
\bar{h}_1{}^\mu{}_{\nu'}(x') &= h_1{}^\mu{}_{\nu'}(x') + B(x')g^\mu{}_{\nu'}\\
\bar{h}_{1\alpha}{}^\mu{}_{\nu'}(x') &= h_{1\alpha}{}^\mu{}_{\nu'}(x')\\
\bar{h}_{1\alpha\beta}{}^\mu{}_{\nu'}(x') &= h_{1\alpha\beta}{}^\mu{}_{\nu'}(x')\\
\bar{h}_2{}^\mu{}_{\nu'}(x') &= h_2{}^\mu{}_{\nu'}(x') + \frac{1}{2}B^2(x')g^\mu{}_{\nu'} + B(x')h_1{}^\mu{}_{\nu'}(x')
\end{aligned} \tag{C3}$$

where $B(x') = -R(x')/6$, $\bar{h}_1{}^\mu{}_{\nu'}(x,x') = \bar{h}_1{}^\mu{}_{\nu'}(x') + \bar{h}_{1\alpha}{}^\mu{}_{\nu'}(x')y^\alpha + \bar{h}_{1\alpha\beta}{}^\mu{}_{\nu'}(x')y^\alpha y^\beta + \mathcal{O}(y^3)$. Here the coefficients $h_j{}^\mu{}_{\nu'}$ can also be found in the literature [82].

As above, we are interested only in terms linear in the Riemann curvature. Using Riemann normal coordinates about x', one obtains

$$G_{\mu\nu'}(x,x') = -\Delta^{1/2}_{\rm VM}(x,x')\int \frac{d^{d_\gamma}k}{(2\pi)^{d_\gamma}} e^{-iky} \times \bar{H}_{\mu\nu'}\left(x,x';-\frac{\partial}{\partial M_\gamma^2}\right)\frac{1}{k^2-M_\gamma^2} \tag{C4}$$

where $M_\gamma^2 = -R(x')/6$ and we used that [81]

$$g_{\mu\nu'}(x,x') = \eta_{\mu\nu'} - \frac{1}{6}R_{\mu\rho\sigma\nu'}(x')y^\rho y^\sigma + \cdots. \tag{C5}$$

By using the aforementioned expansion for the Van Vleck-Morette determinant, together with previous results, one finds that

$$G_{\mu\nu'}(x,x') = -\int \frac{d^{d_\gamma}k}{(2\pi)^{d_\gamma}} e^{-iky}\left[\frac{\eta_{\mu\nu'}}{k^2-M_\gamma^2} + \frac{1}{(k^2-M_\gamma^2)^2}\left(\frac{2}{3}R_{\mu\nu'} - \frac{1}{6}R\eta_{\mu\nu'}\right) - \frac{2}{3}\frac{(2R_{\mu\alpha\beta\nu'} - R_{\alpha\beta}\eta_{\mu\nu'})k^\alpha k^\beta}{(k^2-M_\gamma^2)^3} + \cdots\right]. \tag{C6}$$

Recall that the gauge propagator obtained above corresponds to the one in d_γ dimensions. Since here we are interested in the properties of the system in the reduced space where the fermion field is living, we integrate over the $d_\gamma - d_e$ bulk gauge degrees of freedom.

[1] S. Nadj-Perge, I. K. Drozdov, J. Li, H. Chen, S. Jeon, J. Seo, A. H. MacDonald, B. A. Bernevig, and A. Yazdani, Observation of Majorana fermions in ferromagnetic atomic chains on a superconductor, Science **346**, 602 (2014).

[2] S.-Y. Xu *et al.*, Discovery of a Weyl fermion semimetal and topological Fermi arcs, Science **349**, 613 (2015).

[3] U. Leonhardt and P. Piwnicki, Relativistic Effects of Light in Moving Media with Extremely Low Group Velocity, Phys. Rev. Lett. **84**, 822 (2000); L. J. Garay, J. R. Anglin, J. I. Cirac, and P. Zoller, Sonic Analog of Gravitational Black Holes in Bose-Einstein Condensates, Phys. Rev. Lett. **85**, 4643 (2000); B. Horstmann, B. Reznik, S. Fagnocchi, and J. I. Cirac, Hawking Radiation from an Acoustic Black Hole on an Ion Ring, Phys. Rev. Lett. **104**, 250403 (2010); A. Recati, N. Pavlof, and I. Carusotto, Bogoliubov theory of acoustic Hawking radiation in Bose-Einstein condensates, Phys. Rev. A **80**, 043603 (2009); C. Mayoral, A. Fabbri, and M. Rinaldi, Steplike discontinuities in Bose-Einstein condensates and Hawking radiation: Dispersion effects, Phys. Rev. D **83**, 124047 (2011); G. Menezes and J. Marino, Slow scrambling in sonic black holes, Europhys. Lett. **121**, 60002 (2018).

[4] S. Basak and P. Majumdar, "Superresonance" from a rotating acoustic black hole, Classical Quantum Gravity **20**, 3907 (2003); T. R. Slatyer and C. M. Savage, Superradiant scattering from a hydrodynamic vortex, Classical Quantum Gravity **22**, 3833 (2005); V. Cardoso, A. Coutant, M. Richartz, and S. Weinfurtner, Detecting Rotational Superradiance in Fluid Laboratories, Phys. Rev. Lett. **117**, 271101 (2016); L. Giacomelli and S. Liberati, Rotating black hole solutions in relativistic analogue gravity, Phys. Rev. D **96**, 064014 (2017); D. Faccio and E. M. Wright, Superradiant Amplification of Acoustic Beams via Medium Rotation, Phys. Rev. Lett. **123**, 044301 (2019); M. C. Braidotti, A. Vinante, G. Gasbarri, D. Faccio, and H. Ulbricht, Zel'dovich Amplification in a Superconducting Circuit, Phys. Rev. Lett. **125**, 140801 (2020); L. Giacomelli and I. Carusotto, Ergoregion instabilities in rotating two-dimensional Bose-Einstein condensates: Perspectives on the stability of quantized vortices, Phys. Rev. Research **2**, 033139 (2020); J. Marino, G. Menezes, and I. Carusotto, Zero-point excitation of a circularly moving detector in an atomic condensate and phonon laser dynamical instabilities, Phys. Rev. Research **2**, 042009(R) (2020).

[5] K. Novoselov, A. K. Geim, S. V. Morozov, D. Jiang, M. I. Katsnelson, I. V. Grigorieva, S. V. Dubonos, and A. A. Firsov, Two-dimensional gas of massless Dirac fermions in graphene, Nature (London) **438**, 197 (2005).

[6] Y. Zhang, Y.-W. Tan, H. L. Stormer, and P. Kim, Experimental Observation of Quantum Hall Effect and Berry's Phase in Graphene, Nature (London) **438**, 201 (2005).

[7] K. S. Novoselov, A. K. Geim, S. V. Morozov, D. Jiang, Y. Zhang, S. V. Dubonos, I. V. Grigorieva, and A. A. Firsov, Electric field effect in atomically thin carbon films, Science **306**, 666 (2004).

[8] X. Du, I. Skachko, F. Duerr, A. Luican, and E. Y. Andrei, Fractional quantum Hall effect and insulating phase of Dirac electrons in graphene, Nature (London) **462**, 192 (2009).

[9] K. l. Bolotin, F. Ghahari, M. D. Shulman, H. L. Stormer, and P. Kim, Observation of the fractional quantum Hall effect in graphene, Nature (London) **462**, 196 (2009).

[10] F. Ghahari, Y. Zhao, P. Cadden-Zimansky, K. Bolotin, and P. Kim, Measurement of the $\nu = 1/3$ Fractional Quantum Hall Energy Gap in Suspended Graphene, Phys. Rev. Lett. **106**, 046801 (2011).

[11] C. R. Dean, A. F. Young, P. Cadden-Zimansky, L. Wang, H. Ren, K. Watanabe, T. Taniguchi, P. Kim, J. Hone, and K. L. Shepard, Multicomponent fractional quantum Hall effect in graphene, Nat. Phys. **7**, 693 (2011).

[12] M. S. Foster and I. L. Aleiner, Graphene via large N: A renormalization group study, Phys. Rev. B **77**, 195413 (2008).

[13] Y. Seo, G. Song, P. Kim, S. Sachdev, and S.-J. Sin, Holography of the Dirac Fluid in Graphene with Two Currents, Phys. Rev. Lett. **118**, 036601 (2017).

[14] A. Iorio and G. Lambiase, The Hawking-Unruh phenomenon on graphene, Phys. Lett. B **716**, 334 (2012).

[15] A. Iorio and G. Lambiase, Quantum field theory in curved graphene space-times, Lobachevsky geometry, Weyl symmetry, Hawking effect, and all that, Phys. Rev. D **90**, 025006 (2014).

[16] M. Cvetic and G.W Gibbons, Graphene and the Zermelo optical metric of the BTZ black hole, Ann. Phys. (Amsterdam) **327**, 2617 (2012).

[17] F. de Juan, A. Cortijo, and M. A. H. Vozmediano, Charge inhomogeneities due to smooth ripples in graphene sheets, Phys. Rev. B **76**, 165409 (2007).

[18] A. Cortijo and M. A. H. Vozmediano, Effects of topological defects and local curvature on the electronic properties of planar graphene, Nucl. Phys. **B763**, 293 (2007).

[19] A. Iorio and P. Pais, Revisiting the gauge fields of strained graphene, Phys. Rev. D **92**, 125005 (2015).

[20] E. Arias, A. R. Hernández, and C. Lewenkopf, Gauge fields in graphene with nonuniform elastic deformations: A quantum field theory approach, Phys. Rev. B **92**, 245110 (2015).

[21] M. A. H. Vozmediano, M. I. Katsnelson, and F. Guinea, Gauge fields in graphene, Phys. Rep. **496**, 109 (2010).

[22] X. Du, I. Skachko, A. Barker, and E. Y. Andrei, Approaching ballistic transport in suspended graphene, Nat. Nanotechnol. **3**, 491 (2008).

[23] S. Teber, Field theoretic study of electron-electron interaction effects in Dirac liquids. Ph.D. thesis, 2018, arXiv:1810.08428.

[24] E. C. Marino, Quantum electrodynamics of particles on a plane and the Chern-Simons theory, Nucl. Phys. **B408**, 551 (1993).

[25] E. V. Gorbar, V. P. Gusynin, and V. A. Miransky, Dynamical chiral symmetry breaking on a brane in reduced QED, Phys. Rev. D **64**, 105028 (2001).

[26] E. C. Marino, L. O. Nascimento, V. S. Alves, and C. M. Smith, Interaction Induced Quantum Valley Hall Effect in Graphene, Phys. Rev. X **5**, 011040 (2015).

[27] S. Teber, Electromagnetic current correlations in reduced quantum electrodynamics, Phys. Rev. D **86**, 025005 (2012).

[28] D. Dudal, A. J. Mizher, and P. Pais, Remarks on the Chern-Simons photon term in the QED description of graphene, Phys. Rev. D **98**, 065008 (2018).

[29] D. Dudal, A. J. Mizher, and P. Pais, Exact quantum scale invariance of three-dimensional reduced QED theories, Phys. Rev. D **99**, 045017 (2019).

[30] J. B. Cuevas, A. Raya, and J. C. Rojas, Chiral symmetry restoration in reduced QED at finite temperature in the supercritical coupling regime, Phys. Rev. D **102**, 056020 (2020).
[31] J. A. C. Olivares, L. Albino, A. J. Mizher, and A. Raya, Influence of a Chern-Simons term in the dynamical fermion masses in reduced or pseudo QED, Phys. Rev. D **102**, 096023 (2020).
[32] N. D. Birrell and P. C. W. Davies, *Quantum Fields in Curved Space* (Cambridge University Press, Cambridge, England, 1982).
[33] L. Parker and D. Toms, *Quantum Field Theory in Curved Space-Time* (Cambridge University Press, Cambridge, England, 2009).
[34] A. Z. Petrov, *Einstein Spaces* (Pergamon, Oxford, 1969).
[35] L. Parker, in *Proceedings of the NATO Advanced Study Institute on Gravitation: Recent Developments*, edited by M. Levy and S. Deser (Plenum, New York, 1979).
[36] V. S. Alves, W. S. Elias, L. O. Nascimento, V. Juričić, and F. Peña, Chiral symmetry breaking in the pseudo-quantum electrodynamics, Phys. Rev. D **87**, 125002 (2013).
[37] J.Gonzalez, F. Guinea, and M. A. H.Vozmediano, Non-fermi liquid behavior of electrons in the half-filled honeycomb lattice (A renormalization group approach), Nucl. Phys. **B424**, 595 (1994).
[38] G. de Berredo-Peixoto and I. L. Shapiro, On the renormalization of CPT/Lorentz violating QED in curved space, Phys. Lett. B **642**, 153 (2006).
[39] B. Gonçalves, G. de Berredo-Peixoto, and I. L. Shapiro, One-loop corrections to the photon propagator in the curved-space QED, Phys. Rev. D **80**, 104013 (2009).
[40] B. Gonçalves, G. de Berredo-Peixoto, and I. L. Shapiro, Exact formfactors in the one-loop curved-space QED and the nonlocal multiplicative anomaly, Int. J. Mod. Phys. A **25**, 2382 (2010).
[41] I. L. Buchbinder, S. D. Odintsov, and I. L. Shapiro, *Effective Action in Quantum Gravity* (IOP, Bristol, England, 1992).
[42] P. Panangaden, One-loop renormalization of quantum electrodynamics in curved space-time, Phys. Rev. D **23**, 1735 (1981).
[43] T. S. Bunch and L. Parker, Feynman propagator in curved space-time: A momentum-space representation, Phys. Rev. D **20**, 2499 (1979).
[44] A. O. Barvinsky and G. A. Vilkovisky, The generalized Schwinger-Dewitt technique in gauge theories and quantum gravity, Phys. Rep. **119**, 1 (1985).
[45] I. L. Shapiro, Effective action of vacuum: Semiclassical approach, Classical Quantum Gravity **25**, 103001 (2008).
[46] L. Parker and D. J. Toms, Renormalization-group analysis of grand unified theories in curved space-time, Phys. Rev. D **29**, 1584 (1984).
[47] J. C. Collins, Structure of counterterms in dimensional regularization, Nucl. Phys. **B80**, 341 (1974).
[48] T. S. Bunch, Local momentum space and two-loop renormalizability of $\lambda\phi^4$ field theory in curved space-time, Gen. Relativ. Gravit. **13**, 711 (1981).
[49] M. O. Katanaev and I. V. Volovich, Theory of defects in solids and three-dimensional gravity, Ann. Phys. (Amsterdam) **216**, 1 (1992).
[50] V. A. De Lorenci, R. Klippert, and E. S. Moreira, Jr., Semiclassical backreaction around a cosmic dislocation, Phys. Rev. D **71**, 024005 (2005).
[51] V. A. De Lorenci and E. S. Moreira, Jr., A note on the geometry of a cylindrical shell with screw dislocation, Phys. Lett. A **376**, 2281 (2012).
[52] A. Fasolino, J. H. Los, and M. I. Katsnelson, Intrinsic ripples in graphene, Nat. Mater. **6**, 858 (2007).
[53] V. A. De Lorenci, R. D. M. De Paola, and N. F. Svaiter, From spinning to non-spinning cosmic string spacetime, Classical Quantum Gravity **16**, 3047 (1999).
[54] D. D. Sokoloff and A. A. Starobinsky, On the structure of curvature tensor on conical singularities, Dokl. Akad. Nauk SSSR **234**, 1043 (1977) [Sov. Phys. Dokl. **22**, 312 (1977)].
[55] C. A. de Lima Ribeiro, C. Furtado, and F. Moraes, On the localization of electrons and holes by a disclination core, Phys. Lett. A **288**, 329 (2001).
[56] B. Allen and A. C. Ottewill, Effects of curvature couplings for quantum fields on cosmic-string space-times, Phys. Rev. D **42**, 2669 (1990).
[57] E. A. Kochetov and V. A. Osipov Dirac fermions on a disclinated flexible surface, Pis'ma Zh. Eksp. Teor. Fiz. **91**, 128 (2010) [JETP Lett. **91**, 110 (2010)].
[58] E. A. Kochetov, V. A. Osipov, and R. Pincak, Electronic properties of disclinated flexible membrane beyond the inextensional limit: Application to graphene, J. Phys. Condens. Matter **22**, 395502 (2010).
[59] E. V. Castro, A. Flachi, P. Ribeiro, and V. Vitagliano, Symmetry Breaking and Lattice Kirigami, Phys. Rev. Lett. **121**, 221601 (2018).
[60] A. Flachi and V. Vitagliano, Symmetry breaking and lattice kirigami: finite temperature effects, Phys. Rev. D **99**, 125010 (2019).
[61] S. N. Solodukhin, Conical singularity and quantum corrections to the entropy of a black hole, Phys. Rev. D **51**, 609 (1995).
[62] S. N. Solodukhin, Entanglement entropy of black holes, Living Rev. Relativity **14**, 8 (2011).
[63] G. Oliveira-Neto, Identifying conical singularities, J. Math. Phys. (N.Y.) **37**, 4716 (1996).
[64] D. V. Fursaev, Spectral geometry and one-loop divergences on manifolds with conical singularities, Phys. Lett. B **334**, 53 (1994).
[65] E. A. Mooers, Heat kernel asymptotics on manifolds with conic singularities, J. Anal. Math. **78**, 1 (1999).
[66] M. A. H.Vozmediano, Renormalization group aspects of graphene, Phil. Trans. R. Soc. A **369**, 2625 (2011).
[67] S. Das Sarma, E. H. Hwang, and W.-K. Tse, Many-body interaction effects in doped and undoped graphene: Fermi liquid versus non-Fermi liquid, Phys. Rev. B **75**, 121406(R) (2007).
[68] J. F. Donoghue and B. K. El-Menoufi, Nonlocal quantum effects in cosmology: Quantum memory, nonlocal FLRW equations, and singularity avoidance, Phys. Rev. D **89**, 104062 (2014).
[69] G. L. Klimchitskaya and V. M. Mostepanenko, Quantum electrodynamic approach to the conductivity of gapped graphene, Phys. Rev. B **94**, 195405 (2016).
[70] G. L. Klimchitskaya, V. M. Mostepanenko, and V. M. Petrov, Conductivity of graphene in the framework of Dirac

model: Interplay between nonzero mass gap and chemical potential, Phys. Rev. B **96**, 235432 (2017).
[71] T. Ando, Y. Zheng, and H. Suzuura, Dynamical conductivity and zero-mode anomaly in honeycomb lattices, J. Phys. Soc. Jpn. **71**, 1318 (2002).
[72] A. Iorio and P. Pais, (Anti-)de Sitter, poincare, super symmetries, and the two Dirac points of graphene, Ann. Phys. (Amsterdam) **398**, 265 (2018).
[73] M. F. Ciappina, A. Iorio, P. Pais, and A. Zampeli, Torsion in quantum field theory through time-loops on Dirac materials, Phys. Rev. D **101**, 036021 (2020).
[74] D. J. Toms, Local momentum space and the vector field, Phys. Rev. D **90**, 044072 (2014).
[75] T. Inagaki, T. Muta, and S. D. Odintsov, Nambu-Jona-Lasinio model in curved space-time, Mod. Phys. Lett. A **08**, 2117 (1993).
[76] D. J. Toms, Effective action for the Yukawa model in curved space-time, J. High Energy Phys. 05 (2018) 139.
[77] I. Jack and L. Parker, Proof of summed form of proper-time expansion for propagator in curved space-time, Phys. Rev. D **31**, 2439 (1985).
[78] B. S. DeWitt, in *Relativity, Groups and Topology*, edited by C. DeWitt and B. S. DeWitt (Gordon and Breach, New York, 1964); C. DeWitt and B. S. DeWitt*Dynamical Theory of Groups and Fields* (Gordon and Breach, New York, 1965).
[79] J. H. Van Vleck, The correspondence principle in the statistical interpretation of quantum mechanics, Proc. Natl. Acad. Sci. U.S.A. **14**, 178 (1928); C. Morette, On the definition and approximation of Feynman's path integrals, Phys. Rev. **81**, 848 (1951).
[80] I. L. Buchbinder and S. D. Odintsov, One-loop renormalization of the Yang-mills field theory in a curved space-time, Sov. Phys. J. **26**, 359 (1983).
[81] E. Calzetta, I. Jack, and L. Parker, Quantum gauge fields at high curvature, Phys. Rev. D **33**, 953 (1986).
[82] S. M. Christensen, Regularization, renormalization, and covariant geodesic point separation, Phys. Rev. D **17**, 946 (1978).